

Wilfried Sailer-Kronlachner, BSc

**Synthesis of pyrazolo[3,4-*d*]pyrimidines and  
development of a human xanthine oxidase activity  
test**

Master Thesis

Thesis submitted to the faculty of Technical Chemistry, Chemical and  
Process Engineering, Biotechnology in partial fulfillment of the requirements  
for the degree of

*Master of Science*

in chemistry at Graz University of Technology.

Supervisor:

Ao.Univ.-Prof. Dr.phil. Norbert Klempier

Institute of Organic Chemistry

Graz University of Technology

Graz, Oktober 2017

## EIDESSTÄTLICHE ERKLÄRUNG

Ich erkläre an Eides statt, dass ich die vorliegende Arbeit selbstständig verfasst, andere als die angegebenen Quellen/Hilfsmittel nicht benutzt, und die den benutzten Quellen wörtlich und inhaltlich entnommene Stellen als solche kenntlich gemacht habe. Das in TUGRAZonline hochgeladene Textdokument ist mit der vorliegenden Masterarbeit identisch.

Graz, ..... ..

(Unterschrift)

## STATUTORY DECLARATION

I declare that I have authored this thesis independently, that I have not used other than the declared sources / resources, and that I have explicitly marked all material which has been quoted either literally or by content from the used sources. The document uploaded in TUGRAZonline is identical with the present master thesis.

Graz, ..... ..

(signature)

*„Was man zu verstehen gelernt hat, fürchtet man nicht mehr.“*

*Marie Curie (1867-1934)*

## Danksagung

Als erstes möchte ich mich bei meinem Betreuer, Ao.Univ.-Prof. Dr.phil. Norbert Klempier, bedanken. Er hat mir das Verfassen dieser Arbeit am Institut für organische Chemie ermöglicht und ist mir während der gesamten Zeit meiner Diplomarbeit immer mit Rat und Tat zur Seite gestanden. Seine stets hilfreiche und kompetente Art hat mir die Arbeit sehr erleichtert.

Außerdem gilt mein Dank Dipl.-Ing. Dr.techn. Birgit Wilding, die mich mit viel Elan durch die Zeit meiner Masterarbeit begleitet und mir vor allem bei der praktischen Arbeit im Labor und in Planungsfragen stets eine große Hilfe war.

Meinen Dank möchte ich auch allen Mitarbeitern/innen am Institut für organische Chemie aussprechen, die mir während meiner Zeit am Institut in allen möglichen Fragen stets eine große Hilfe waren und eine freundschaftliche und angenehme Arbeitsatmosphäre geschaffen haben.

Mein größter Dank gilt meinen Eltern Monika und Norbert Sailer-Kronlachner, die mir dieses Studium ermöglicht und mich auch in schwierigen Phasen stets unterstützt und wieder motiviert haben. Weiters möchte ich auch meinen Geschwistern Barbara und Wolfgang danken, die immer an mich geglaubt haben und mir dadurch die nötige Kraft gegeben haben dieses Studium zu beenden.

Weiters möchte ich mich bei allen Freunden/innen und Studienkollegen/innen bedanken, die meine Studienzzeit zu einer Zeit gemacht haben an die ich immer gerne zurück denken werde. Besonders hervorheben möchte ich hier Elisabeth Verwüster, Stefan Nestl, Alex Schenk, Sebastian Schweiger, Andi Kautsch und Sebastian Haid. Ich weiß nicht ob ich ohne euch dieses Studium beendet hätte, vielen Dank dass ihr mit mir auch die schweren oder frustrierenden Phasen des Studiums durchlebt habt.

## Abstract

Pyrazolo[3,4-*d*]pyrimidines display a wide variety of biological activities. This is due to their structural resemblance to purines, which prompted the investigation of their therapeutic significance. Pyrazolo[3,4-*d*]pyrimidines like Allopurinol or Ibrutinib are examples for the importance of these compounds, since they are used today in the treatment of chronic gout (Allopurinol) and lymphomas (Ibrutinib).

In this master thesis, a series of pyrazolo[3,4-*d*]pyrimidines was synthesized. The targeted compounds were prepared using a synthesis approach that starts with the preparation of appropriately functionalized pyrazole precursors.

The synthesized pyrazolo[3,4-*d*]pyrimidines are of interest as substrates for two different enzymes, xanthine oxidase and nitril reductase queF and will be used to explore their substrate scope.

Xanthine oxidase catalyzes the last two steps of the purine degradation in mammals, the oxidation from hypoxanthine to uric acid. Most of the work on xanthine oxidase found in literature is focused on its inhibition, because of its importance in the treatment in a series of illnesses, e.g. gout.

The second part of this master thesis was the development of an activity test for a specific human milk xanthine oxidase whole cell preparation.

## Kurzfassung

Pyrazolo[3,4-*d*]pyrimidine zeigen eine Vielzahl biologischer Aktivitäten, ausgelöst durch ihre strukturelle Ähnlichkeit zu Purinen. Diese Ähnlichkeit führte zur Untersuchung ihrer therapeutischen Signifikanz. Pyrazolo[3,4-*d*]pyrimidine wie Allopurinol oder Ibrutinib sind Beispiele für die Relevanz dieser Verbindungen da sie heute als Medikamente zur Behandlung von Gicht (Allopurinol) und Lymphomen (Ibrutinib) eingesetzt werden.

In dieser Masterarbeit wurde eine Reihe von Pyrazolo[3,4-*d*]pyrimidinen mittels eines Synthesansatzes hergestellt, der mit der Synthese von korrekt funktionalisierten Pyrazolen als Ausgangsstoffe beginnt.

Die synthetisierten Pyrazolo[3,4-*d*]pyrimidine sind als Substrate für zwei verschiedene Enzyme, Xanthine Oxidase und Nitril Reductase queF, interessant. Die Verbindungen wurden zur Erforschung der Substratspektren dieser Enzyme eingesetzt.

Xanthine Oxidase katalysiert die letzten zwei Reaktionsschritte des Purinabbaus in Säugetieren, also die Oxidation von Hypoxanthin zu Harnsäure. Der überwiegende Teil der Literatur die bisher über Xanthine Oxidase veröffentlicht wurde beschäftigt sich mit der Inhibition dieses Enzymes, da die Inhibition von Xanthine Oxidase eine Rolle in der Behandlung einer Reihe von Krankheiten, wie zum Beispiel Gicht, spielt.

Der zweite Teil dieser Masterarbeit beschäftigt sich mit der Entwicklung eines Aktivitätstests für eine spezifische Ganzzellen-Präparation menschlicher Xanthine Oxidase.

## Table of Contents

<b>Danksagung</b> .....	<b>IV</b>
<b>Abstract</b> .....	<b>V</b>
<b>Kurzfassung</b> .....	<b>VI</b>
<b>1 Aim of this work</b> .....	<b>3</b>
<b>2 Introduction</b> .....	<b>5</b>
<b>2.1 Pyrazolo[3,4-<i>d</i>]pyrimidines</b> .....	<b>5</b>
2.1.1 Nomenclature of pyrazolopyrimidines .....	5
2.1.2 Synthesis of pyrazolo[3,4- <i>d</i> ]pyrimidines.....	6
2.1.2.1 Syntheses using pyrazole precursors.....	6
2.1.2.1.1 Synthesis of the pyrimidine ring .....	7
2.1.2.1.2 Introduction of substituents in position 1 and 3 of pyrazolo[3,4- <i>d</i> ]pyrimidines .....	10
2.1.2.2 Synthesis using pyrimidine precursors .....	12
2.1.3 Bioactivity of pyrazolo[3,4- <i>d</i> ]pyrimidines .....	13
2.1.3.1 Xanthine oxidase inhibition.....	13
2.1.3.2 Antitumor activity.....	15
2.1.3.3 Other biological activities .....	16
<b>2.2 Xanthine Oxidase</b> .....	<b>17</b>
2.2.1 Structure of xanthine oxidase .....	18
2.2.2 Reaction mechanism of xanthine oxidase.....	20
2.2.3 Substrate scope and Inhibition of xanthine oxidase .....	21
2.2.3.1 Substrate scope of xanthine oxidase.....	21
2.2.3.2 Inhibition of xanthine oxidase .....	24

<b>3 Results and Discussion .....</b>	<b>26</b>
<b>3.1 Synthesis of the targeted pyrazolo[3,4-<i>d</i>]pyrimidines .....</b>	<b>26</b>
<b>3.2 Xanthine oxidase activity test .....</b>	<b>42</b>
<b>4 Conclusion and outlook.....</b>	<b>50</b>
<b>5 Experimental .....</b>	<b>52</b>
<b>5.1 General Methods.....</b>	<b>52</b>
5.1.1 Thin Layer Chromatography .....	52
5.1.2 Column Chromatography.....	52
5.1.3 High Performance Liquid Chromatography .....	52
5.1.4 Nuclear Magnetic Resonance Spectroscopy .....	54
5.1.5 Biotransformations.....	55
<b>5.2 Synthesis of pyrazolo[3,4-<i>d</i>]pyrimidines.....</b>	<b>56</b>
<b>6 References .....</b>	<b>64</b>
<b>7 Appendix .....</b>	<b>68</b>
List of Abbreviations .....	68
List of Schemes .....	68
List of Figures .....	70
List of Tables.....	72



## 1 Aim of this work

The aim of the first part of this master thesis was the synthesis of a series of pyrazolo[3,4-*d*]pyrimidines. The pyrazolo[3,4-*d*]pyrimidine nucleus (Figure 1) is an important drug-like scaffold that is present in many pharmacologically active compounds. This is due to their structural resemblance to purines which prompted biological investigations of their therapeutic significance as drugs with the potential to modulate purine activity or metabolism.<sup>[1]</sup>

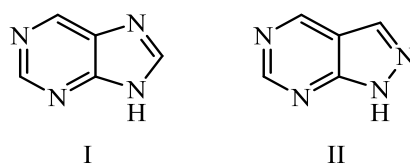
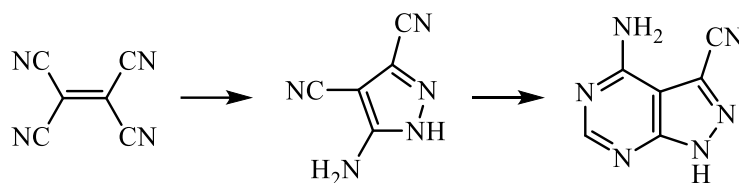


**Figure 1. (I) purine scaffold; (II) pyrazolo[3,4-*d*]pyrimidine scaffold**

Pyrazolo[3,4-*d*]pyrimidines are prepared through 2 different pathways, starting either from pyrimidine- or from pyrazole precursors. For this thesis, the targeted compounds were synthesized using correctly substituted pyrazole precursors, as can be seen in Scheme 1.



**Scheme 1. Example of a synthesis scheme used in the preparation of the targeted compounds**

The synthesized pyrazolo[3,4-*d*]pyrimidines are possible substrates of xanthine oxidase (XO), the enzyme responsible for the last two steps in purine degradation.<sup>[2]</sup>

The second part of this thesis was the development of an activity test for a specific whole cell preparation of a human xanthine oxidase expressing *E. coli* strain. It is important to note that human milk XO was used in this thesis, because most of the work on XO was done with enzymes from other sources (mostly bovine milk).

Most of the work on XO found in literature is dealing with the inhibitory effect of a broad variety of substances. In this work, we wanted to find a reliable activity testing system for human XO using HPLC analysis. The prepared pyrazolo[3,4-*d*]pyrimidines will then be tested as possible substrates of XO.

Some of the prepared compounds were also used by this working group in the investigation of the substrate scope of a novel enzyme, nitrile reductase queF. This enzyme is able to reduce a nitrile function to its corresponding primary amine and is part of the biosynthetic pathway to queuosine.<sup>[3]</sup>

## 2 Introduction

### 2.1 Pyrazolo[3,4-*d*]pyrimidines

Pyrazolo[3,4-*d*]pyrimidines display a wide range of biological activities. Their structural resemblance to purines prompted biological investigations of their therapeutic significance. The pyrazolo[3,4-*d*]pyrimidine nucleus (Figure 2) is an important drug-like scaffold that is present in many pharmacologically active compounds. The continuing interest in pyrazolo[3,4-*d*]pyrimidine derivatives as drugs with the potential to modulate purine activity or metabolism leads to new approaches for the synthesis of these derivatives.<sup>[1]</sup> This chapter surveys nomenclature, synthesis and bioactivity of pyrazolo[3,4-*d*]pyrimidines.

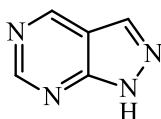


Figure 2. 1*H*-pyrazolo[3,4-*d*]pyrimidine

#### 2.1.1 Nomenclature of pyrazolopyrimidines

The parent structure of the condensed ring system is the pyrimidine ring (III). The numbering according to IUPAC nomenclature can be seen in Figure 3.

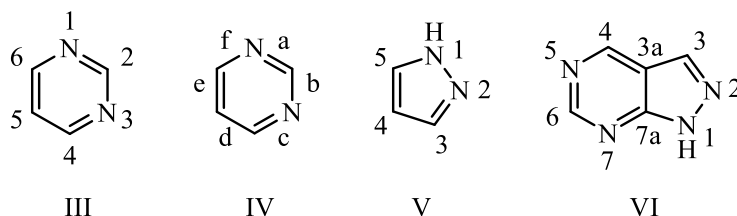


Figure 3. Numbering of the pyrazolopyrimidine system and its main compounds

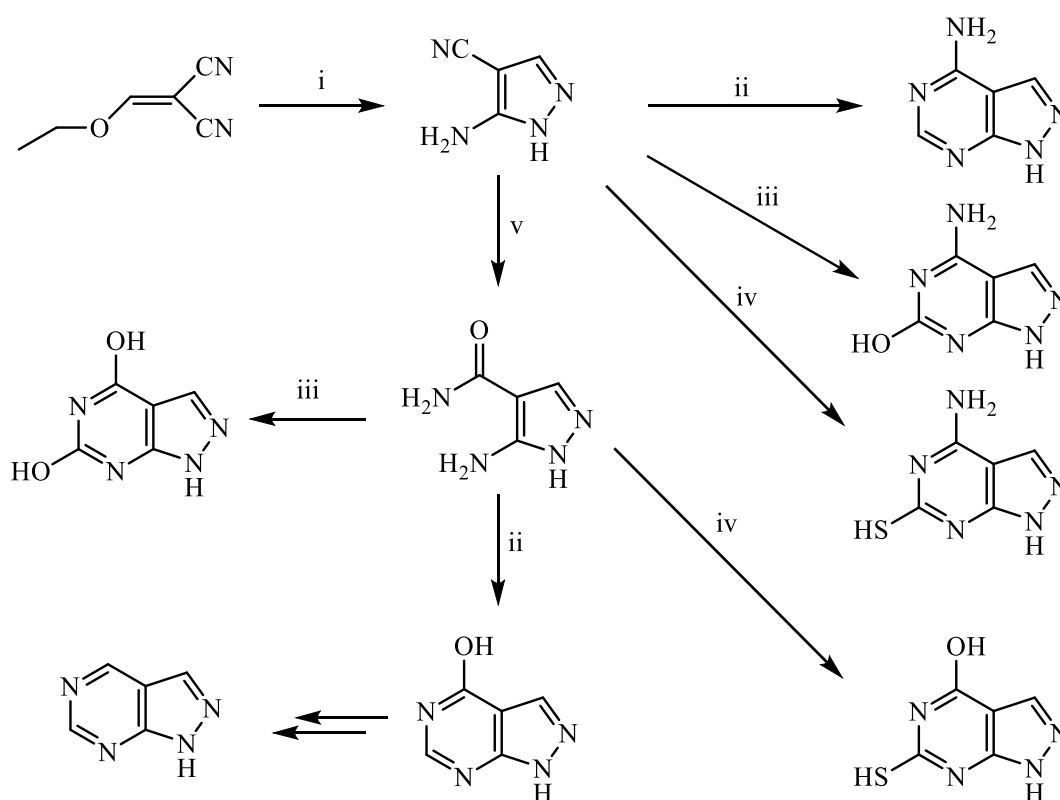
Italic letters are assigned to the bonds alphabetically (IV) to determine the bond connecting the pyrimidine ring to the smaller pyrazole moiety. The bond of the pyrazole ring (V) that is connected to the pyrimidine ring is determined by the numbers assigned to the bridge atoms in the uncondensed pyrazole. These numbers and letters are written in brackets prior to the parent compounds name.<sup>[4]</sup> Therefore the condensed system (VI) that can be seen in Figure 3 is named 1*H*-pyrazolo[3,4-*d*]pyrimidine. It is then numbered starting from the pyrazole moiety.

## 2.1.2 Synthesis of pyrazolo[3,4-*d*]pyrimidines

Beginning with the work of Robins<sup>[5]</sup> in the 1950s, researchers have dedicated much effort to investigating new approaches for the synthesis of pyrazolo[3,4-*d*]pyrimidine derivatives. There are two main strategies found in literature to build up the pyrazolo[3,4-*d*]pyrimidine scaffold, the first starting from the pyrazole moiety and the second starting from the pyrimidine moiety. Variations of these two routes to the condensed system are described hereafter.

### 2.1.2.1 Syntheses using pyrazole precursors

Robins synthesized differently substituted pyrazolo[3,4-*d*]pyrimidines starting from ethoxymethylene malonitrile. Reaction with hydrazine monohydrate and subsequently sulfuric acid produced pyrazole precursors which were used in condensation reactions with urea, formamide and thiourea to form 1,2-unsubstituted pyrazolo[3,4-*d*]pyrimidines. Substituents in positions 4 and 6 were altered using e.g. chlorination with phosphorus oxychloride followed by hydration or selective replacement reactions with different amines to get to another batch of 1,2-unsubstituted pyrazolo[3,4-*d*]pyrimidines.<sup>[5]</sup>



**Scheme 2. Robins path to 1,2-unsubstituted pyrazolo[3,4-*d*]pyrimidines; (i)  $\text{NH}_2\text{NH}_2$ , EtOH, reflux; (ii)  $\text{HCONH}_2$ , reflux; (iii)  $\text{NH}_2\text{CONH}_2$ , 180-200°C; (iv)  $\text{NH}_2\text{CSNH}_2$ , 180°C**

### 2.1.2.1.1 Synthesis of the pyrimidine ring

Some approaches to the formation of the two ring system are quite similar to this first approach by Robins. There are basically three different substituents in position 4 used to build up the pyrimidine ring, which can be seen in Figure 4.

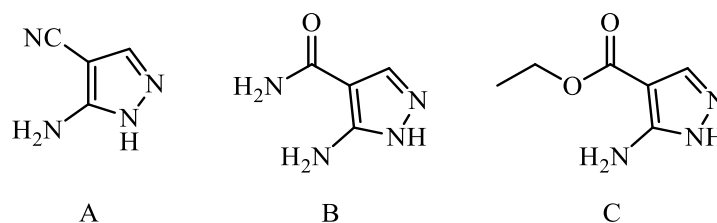
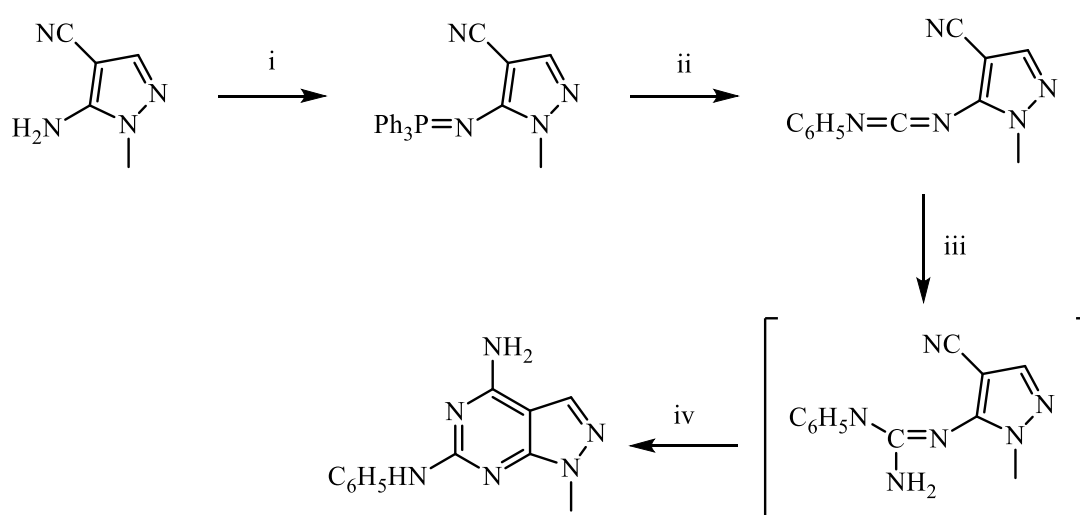


Figure 4. Different substituents used to build up the pyrimidine moiety

Use of pyrazole (A) leads to the formation of an amino substituent in position 4 of the condensed system whereas the amide (B) and carboxylate (C) lead to a keto or hydroxy group.

A variety of different methods for the formation of the pyrimidine moiety is found in the literature. Substituents in position 6 of the condensed system depend on the used reactants and method in the condensation reaction. The reaction with formamide e.g. leads to the formation of 6-unsubstituted pyrazolopyrimidines whereas the reactions with urea, thiourea or guanidine carbonate lead to the corresponding hydroxyl, mercapto and amino derivatives.<sup>[5][6][7]</sup>

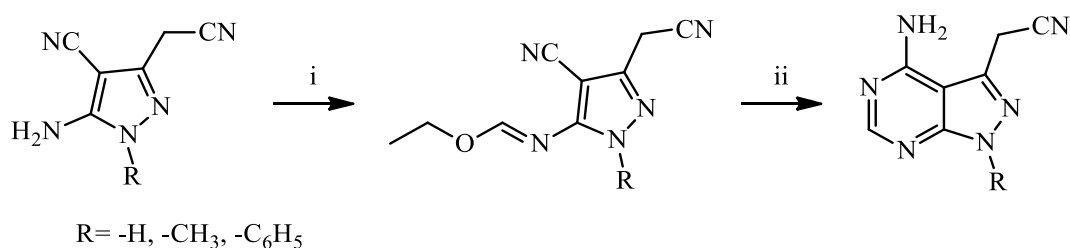
Another approach can be seen in Scheme 3.



Scheme 3. Synthesis of 6-phenylamino-substituted pyrazolo[3,4-d]pyrimidines; (i)  $\text{PPh}_3$ ,  $\text{Br}_2$ , TEA, 0-25°C; (ii) phenyl isocyanate, THF, 25°C; (iii)  $\text{NH}_3$ , THF, r.t. ; (iv) MeOH, reflux

In situ generated dibromotriphenylphosphorane is reacted with pyrazoles of variants A or C to build up iminophosphoranes which undergo aza-Wittig reaction with phenyl isocyanate to produce carbodiimides. Treatment with ammonia and subsequent heating in methanol or ethanol gives, via the guanidine intermediates, the targeted 6-phenylamino-substituted pyrazolo[3,4-*d*]pyrimidines.<sup>[8]</sup>

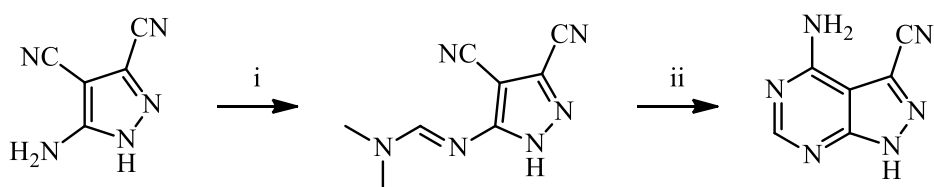
This reaction with phenyl isocyanate is an example for the use of isocyanates or isothiocyanates in the synthesis of the pyrimidine ring. Chlorosulfonyl isocyanate and benzoyl isocyanate can also be used to synthesize differently substituted pyrazolo[3,4-*d*]pyrimidines.<sup>[9][10]</sup> Variant C pyrazole precursors are primarily used in this reaction strategy, whereas there are several other reaction strategies for variants A and B.



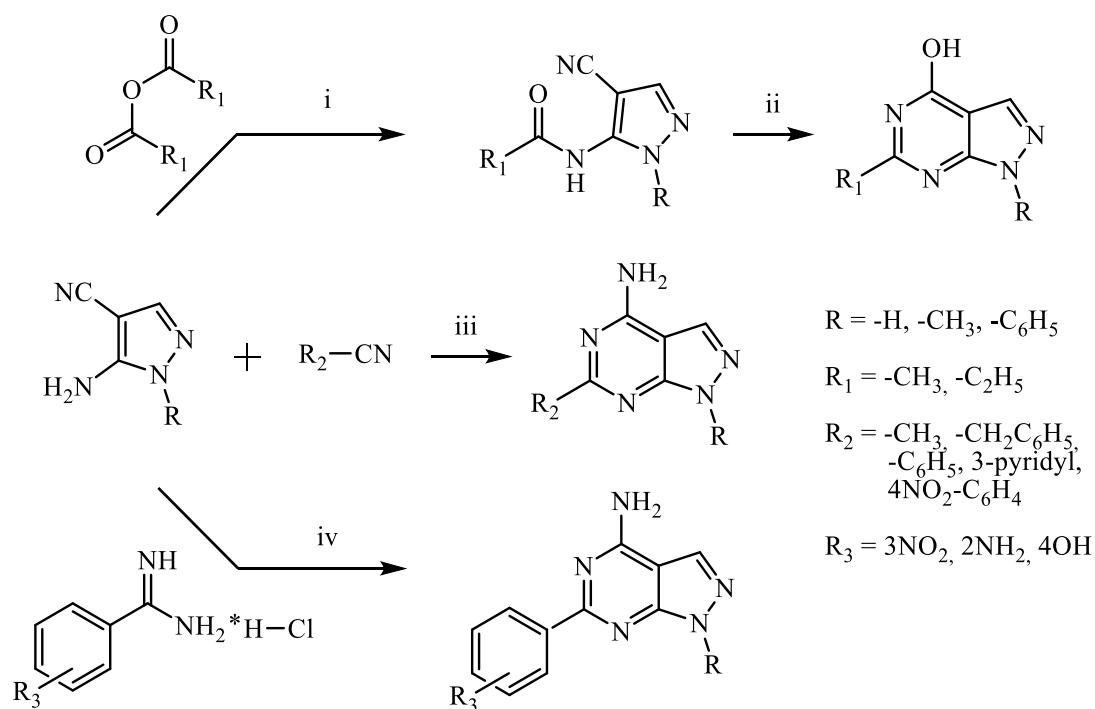
**Scheme 4. Synthesis of 4-amino-3-cyanomethylpyrazolo[3,4-*d*]pyrimidines; (i) (EtO)<sub>3</sub>CH, Ac<sub>2</sub>O, 140°C; (ii) NH<sub>3</sub>/EtOH, rT**

Scheme 4 shows a synthesis using the reaction of pyrazole precursors of variant A with ethyl orthoformate and subsequent reaction with ethanolic ammonia to build up 3-cyano and 3-cyanomethylpyrazolo[3,4-*d*]pyrimidines unsubstituted in position 6.<sup>[11][12]</sup>

A similar approach by Bulychev et al. use dimethylformamide dimethylacetal to build a 5-dimethylaminomethyleneamino pyrazole which is boiled in ammonium hydroxide 20% to build the pyrimidine ring (Scheme 5).<sup>[13]</sup>



**Scheme 5. Bulychev's approach to 3-cyano-4-amino-5-(dimethylaminomethyleneamino)pyrazolo[3,4-*d*]pyrimidines; (i) dimethylformamide dimethylacetal, MeOH abs., reflux temperature; (ii) NH<sub>4</sub>OH 20%, reflux**



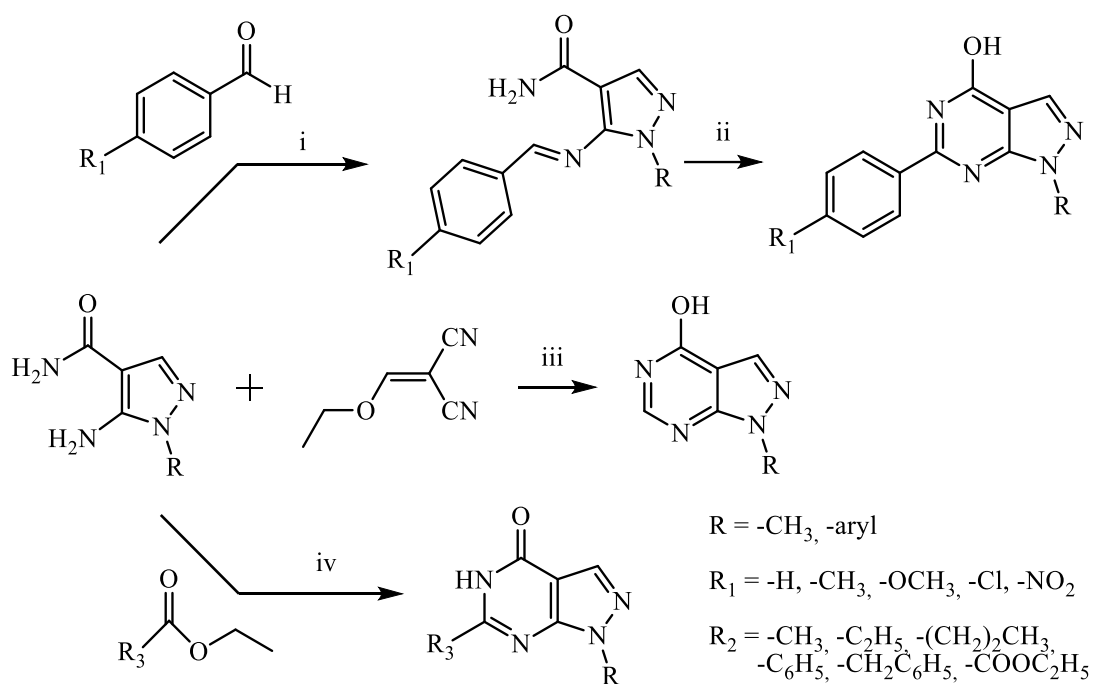
**Scheme 6. Syntheses starting from pyrazole variant A; (i) reflux; (ii) H<sub>2</sub>O<sub>2</sub>, KOH, 75°C; (iii) NH<sub>3</sub>/MeOH, 200°C; (iv) CH<sub>3</sub>COONa, 200°C**

Acylation of 5-amino-4-cyanopyrazoles (A) with organic acid anhydrides results in the formation of 5-acylamino-4-cyanopyrazoles. Subsequent treatment with H<sub>2</sub>O<sub>2</sub> in alkaline solution gives 6-alkyl-4-hydroxypyrazolo[3,4-*d*]pyrimidines (Scheme 6).<sup>[14]</sup> With slightly altered reaction conditions and using TFAA as anhydride, this method can be used to build 6-trifluoromethyl-substituted pyrazolo[3,4-*d*]pyrimidines.<sup>[15]</sup>

Another series of different pyrazolo[3,4-*d*]pyrimidines can be synthesized by reaction of variant A pyrazoles with different nitriles in methanolic ammonia at 200°C in a hydrogenation bomb (Scheme 6).<sup>[16]</sup> This method was altered by Oliveira-Campos and colleagues in 2008. They used microwave assisted organic synthesis (MAOS) and potassium *tert*-butoxide to introduce different substituents in position 6, including several heterocyclic rings like thiophen or furan.<sup>[17]</sup>

Reaction with substituted benzamidine hydrochlorides and sodium acetate at 200°C can be used to synthesize 6-aryl-substituted derivatives (Scheme 6).<sup>[18]</sup>

Syntheses of pyrazolo[3,4-*d*]pyrimidines using variant B precursors include the use of ethoxymethylene malononitrile to build up 1-substituted 4-hydroxypyrazolo[3,4-*d*]pyrimidines<sup>[19]</sup>, the reaction with different esters and sodium ethoxide to yield 1,6-alkyl/aryl disubstituted pyrazolo[3,4-*d*]pyrimidines<sup>[20]</sup> and the condensation with aromatic aldehydes to arylidenamino pyrazoles with subsequent acidic cyclization (HCl, *p*-TSA).<sup>[21]</sup> These three strategies are depicted in Scheme 7.



**Scheme 7. Syntheses starting from pyrazole variant B; (i) AcOH, r.t. ; (ii) HCl or p-TSA, MeOH, reflux; (iii) DMF, reflux; (iv) C<sub>2</sub>H<sub>5</sub>ONa, EtOH, reflux**

#### 2.1.2.1.2 Introduction of substituents in position 1 and 3 of pyrazolo[3,4-*d*]pyrimidines

Substituents in positions 1 and 3 of the pyrazolo[3,4-*d*]pyrimidine scaffold are in most cases introduced during the synthesis of the pyrazole precursors. Substituents in position 3 are generated through the synthesis of correctly substituted reactants. These reactants are  $\alpha,\beta$ -unsaturated nitriles, ketones, esters and acids.

Substituents in position 1 are introduced by the use of monosubstituted hydrazine derivatives in the ring closure reaction with the above mentioned  $\alpha,\beta$ -unsaturated compounds. Table 1 shows different starting materials and the corresponding pyrazole precursors generated in the reaction with hydrazine derivatives.



Table 1. Overview of reactants and corresponding pyrazole precursors

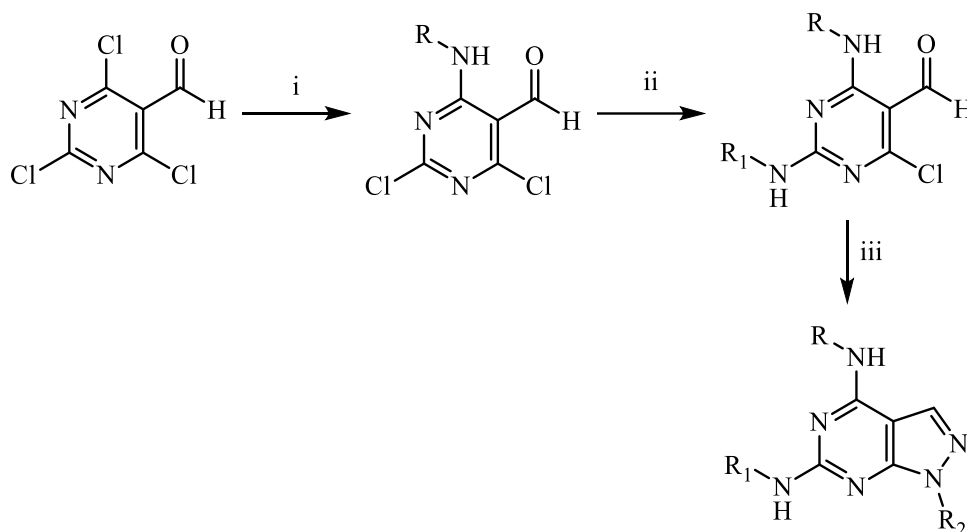
reactant	synthesized precursor	substituents	reference number
		R = H, CH <sub>3</sub> , C <sub>6</sub> H <sub>5</sub> , 4Cl-C <sub>6</sub> H <sub>4</sub>	[5], [22]
		R = H, C <sub>6</sub> H <sub>5</sub>	[23]
		-	[22]
		X = CN, CONH <sub>2</sub> R = H, C <sub>6</sub> H <sub>5</sub> , 4Cl-C <sub>6</sub> H <sub>4</sub> , 4NO <sub>2</sub> -C <sub>6</sub> H <sub>4</sub>	[6]
		X = CN, CONH <sub>2</sub> R = H, C <sub>6</sub> H <sub>5</sub> , 4Cl-C <sub>6</sub> H <sub>4</sub> , 4NO <sub>2</sub> -C <sub>6</sub> H <sub>4</sub> Ar = C <sub>6</sub> H <sub>5</sub> , 4Cl-C <sub>6</sub> H <sub>4</sub> 4CH <sub>3</sub> O-C <sub>6</sub> H <sub>4</sub>	[6]
		R = H, CH <sub>3</sub> , C <sub>6</sub> H <sub>5</sub> , CH <sub>3</sub> CO, C <sub>6</sub> H <sub>5</sub> CO, C <sub>6</sub> H <sub>5</sub> NHCO, NH <sub>2</sub> CO and others	[12]
		X = 4-morpholino, SCH <sub>3</sub> R = C <sub>6</sub> H <sub>5</sub> , 4CH <sub>3</sub> O-C <sub>6</sub> H <sub>4</sub> , 3,4-(CH <sub>3</sub> O) <sub>2</sub> -C <sub>6</sub> H <sub>3</sub> , 4Cl-C <sub>6</sub> H <sub>4</sub> , CH <sub>2</sub> C <sub>6</sub> H <sub>5</sub> and others R <sub>1</sub> = H, C <sub>6</sub> H <sub>5</sub>	[24]
		ref 1: R = CH <sub>3</sub> , C <sub>6</sub> H <sub>5</sub> , 4Cl-C <sub>6</sub> H <sub>4</sub> , 4CH <sub>3</sub> -C <sub>6</sub> H <sub>4</sub> , 4CH <sub>3</sub> O-C <sub>6</sub> H <sub>4</sub> and others R <sub>1</sub> = CH <sub>3</sub> , (CH <sub>2</sub> ) <sub>2</sub> OH, Aryls ref 2: R = 4Cl-C <sub>6</sub> H <sub>4</sub> -CH <sub>2</sub> , 4Cl-C <sub>6</sub> H <sub>4</sub> , 2,4diCl <sub>2</sub> - C <sub>6</sub> H <sub>3</sub> , 3,4diCl <sub>2</sub> -C <sub>6</sub> H <sub>3</sub> R <sub>1</sub> = H, CH <sub>3</sub>	[7], [25]
		X = CN, CONH <sub>2</sub> R = H, C <sub>6</sub> H <sub>5</sub> , 4Cl-C <sub>6</sub> H <sub>4</sub> , 4NO <sub>2</sub> -C <sub>6</sub> H <sub>4</sub>	[26]
		-	[27]

### 2.1.2.2 Synthesis using pyrimidine precursors

Syntheses starting from the pyrimidine ring are less frequently seen in literature than syntheses starting from the pyrazole moiety. Again, as in the syntheses for the pyrazole precursors, hydrazine derivatives are used to build up the pyrazole ring. Reaction of these hydrazine derivatives with pyrimidine precursors possessing an aldehyde or cyano functionality<sup>[28]</sup> at position 5 and a chloro function either in position 4 or 6 yield the desired pyrazolo[3,4-*d*]pyrimidine scaffold. E.g. reaction of 2-Amino-4,6-dichloro-pyrimidine-5-carbaldehyde with hydrazine hydrate yields 6-amino-4-chloro-1*H*-pyrazolo[3,4-*d*]pyrimidine.<sup>[29]</sup>

Aminations of the same precursor with equimolar amounts of different amines yield *N*<sup>4</sup>-substituted precursors. These precursors are cyclized under microwave irradiation in solvent free conditions.<sup>[30]</sup>

Scheme 8 shows an approach by Slavish et al. who synthesized a library of different pyrazolo[3,4-*d*]pyrimidines starting from 2,4,6-trichloropyrimidine-5-carbaldehyde.<sup>[31]</sup>



**Scheme 8.** Slavish's approach using a pyrimidine precursor; (i) RNH<sub>2</sub>, KHCO<sub>3</sub>, TBAI, DCM or THF/H<sub>2</sub>O, r.t. ; (ii) R<sub>1</sub>NH<sub>2</sub>, KHCO<sub>3</sub>, TBAI, DCM/H<sub>2</sub>O, r.t. ; (iii) R<sub>2</sub>NHNH<sub>2</sub>, THF, reflux

Tetrabutylammonium iodide is used as phase transfer catalyst under basic conditions to react the carbaldehyde precursor with different anilines. The intermediates are subsequently cyclized with hydrazine derivatives.

Another recent approach leading to 1-aryl pyrazolo[3,4-*d*]pyrimidines used 4,6-dichloropyrimidine-5-carbaldehyde and aromatic hydrazines to form hydrazones which were subsequently cyclized using MAOS in acetonitrile at 200°C.<sup>[32]</sup>

### 2.1.3 Bioactivity of pyrazolo[3,4-*d*]pyrimidines

As mentioned above, pyrazolo[3,4-*d*]pyrimidines display a wide range of biological activities. A complete review of these activities would go beyond the scope of this thesis. Therefore, a few examples were chosen to show the wide variety of activities and the importance of these compounds.

#### 2.1.3.1 Xanthine oxidase inhibition

A well-known example of a biologically active pyrazolo[3,4-*d*]pyrimidine is Allopurinol (Zykloprim), depicted in Figure 5. Gertrude Ellion and George H. Hitchings worked on its inhibitory effect on xanthine oxidase (XO). XO is the enzyme responsible for the oxidation of hypoxanthine and xanthine to uric acid. Therefore, Allopurinol is used primarily to treat hyperuricemia (excess uric acid in blood plasma) and chronic gout. Its metabolite Oxypurinol (Figure 5) also is a potent XO inhibitor that binds tightly to the reduced form of XO, thereby inactivating it. Oxypurinol has a longer half life in the blood plasma (18-30 hours) than Allopurinol (90-120 minutes), but is not absorbed completely orally, which is why Allopurinol is used as prodrug for Oxypurinol.<sup>[33]</sup>

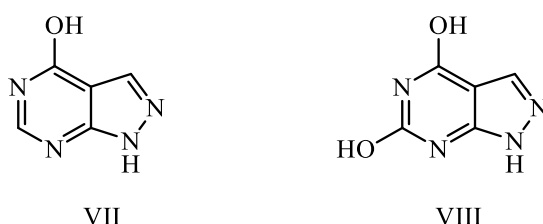
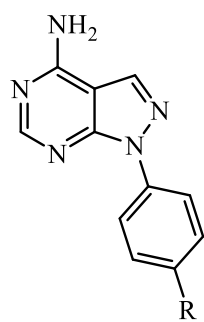


Figure 5. (VII) Allopurinol; (VIII) Oxypurinol

Gertrude Ellion and George H. Hitchings were rewarded the 1988 Nobel Prize for Physiology or Medicine together with James Black for their “discoveries of important principles for drug treatment”. Gupta et al. synthesized a series of other potent pyrazolo[3,4-*d*]pyrimidine XO inhibitors. The strongest effects on XO activity were observed for compounds possessing a glycine methyl ester-, cyano-, nitro- or trifluoromethyl- group bound to an aryl group in position 1 of the pyrazole moiety, exhibiting IC<sub>50</sub> values near or below 2 μM (Allopurinol: IC<sub>50</sub> 24,4 μM).<sup>[34]</sup>



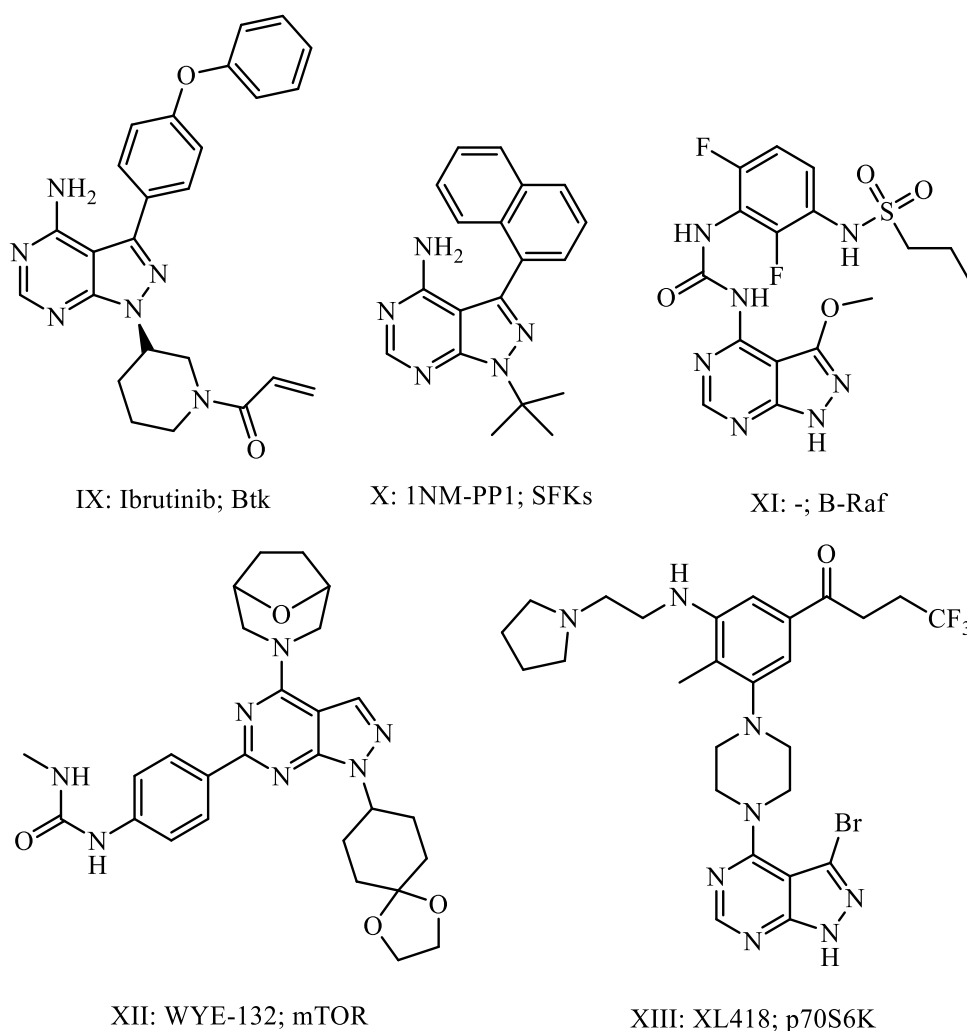
R = -CN, -NO<sub>2</sub>, -CF<sub>3</sub>, -CONHCH<sub>2</sub>CO<sub>2</sub>CH<sub>3</sub>

Figure 6. Structure of XO-inhibitors synthesized by Gupta et al.

### 2.1.3.2 Antitumor activity

The antitumor effect of pyrazolo[3,4-*d*]pyrimidines is primarily dependent on tyrosine or serine/threonine kinase inhibition. In 2014, the pharmaceutical industry spent approximately half of their budget for development on kinases and their inhibitors. An example of a kinase inhibitor containing the pyrazolo[3,4-*d*]pyrimidine scaffold approved by the FDA for the treatment of lymphomas is Ibrutinib (Figure 7).<sup>[1]</sup> It acts as an inhibitor for bruton tyrosin kinase which is part of the B-cell antigen receptor signaling pathway connected to B-cell malignancies.<sup>[35]</sup>

A series of other enzymes connected to various types of cancer is inhibited by a variety of differently substituted pyrazolo[3,4-*d*]pyrimidines. Figure 7 shows some examples of these active compounds and lists their associated inhibited enzyme type.



**Figure 7. Pyrazolo[3,4-*d*]pyrimidines inhibiting various types of enzymes; (IX) Ibrutinib; Btk<sup>[35]</sup> (X) 1NM-PP1; SFKs<sup>[36]</sup> (XI) -, B-Raf<sup>[37]</sup> (XII) WYE-132; mTOR<sup>[38]</sup> (XIII) XL418; p70S6K<sup>[39]</sup>**

### 2.1.3.3 Other biological activities

In addition to their use in cancer and hyperuricemia treatments pyrazolo[3,4-*d*]pyrimidines are also investigated as compounds for pain treatment. Diaz et al. synthesized compounds with acylamino- or cyclic substituents like a pyrazole moiety in position 4 of the pyrazolo[3,4-*d*]pyrimidine scaffold. These compounds displayed potent antinociceptive properties indicating that they act as antagonists to the  $\sigma$ 1-receptor system which is linked to pro-nociception and is located in areas of the body responsible for pain control.<sup>[40][41]</sup>

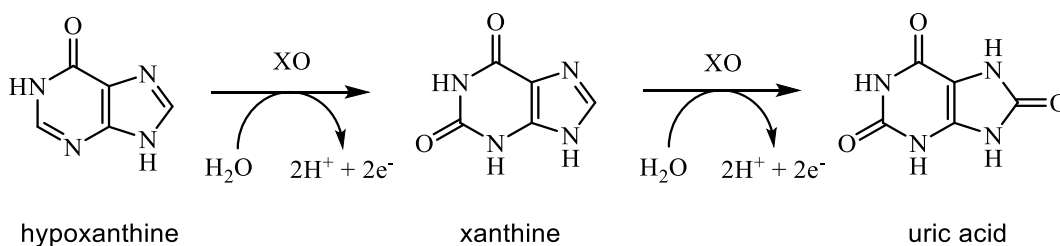
Pyrazolo[3,4-*d*]pyrimidines also display a variety of antimicrobial activities. Beyzaei et al. showed the inhibitory effects of 4-imino-5*H*-pyrazolo[3,4-*d*]pyrimidin-5-amines against gram-positive and gram-negative bacteria<sup>[42]</sup> and Ibrahim et al. reported antibacterial and antifungal effects of 1-phenyl-1*H*-pyrazolo[3,4-*d*]pyrimidine derivatives.<sup>[43]</sup>

These examples show the importance of the pyrazolo[3,4-*d*]pyrimidine scaffold in present day research and in the treatment of various diseases.

## 2.2 Xanthine Oxidase

Xanthine oxidase (XO, EC 1.17.3.2) is a molybdenum containing hydroxylase that catalyzes the last steps of the purine degradation. In mammals, it is one of two interconvertible forms of the enzyme xanthine oxidoreductase, the second one being xanthine dehydrogenase (XDH, EC 1.17.1.4). Xanthine oxidoreductases have been shown to catalyze the hydroxylation of purines, pyrimidines, pterins and aldehydes.<sup>[2]</sup>

The last two steps in the purine catabolism, the oxidation of hypoxanthine to xanthine and of xanthine to uric acid, are depicted in Scheme 9.



**Scheme 9. The last two steps of the purine catabolism; Oxidation of hypoxanthine to uric acid**

Molybdenum hydroxylases were first discovered over a century ago in bovine milk by Schardinger. In 1902, he showed the discoloration of methylene blue by fresh milk when formaldehyde was added, although he did not identify a molybdenum containing enzyme as cause of this reaction. Mostly pure samples of XO were obtained by Ball and by Corran et al. in 1939. The enzyme has been studied intensively since then.<sup>[44]</sup>

Molybdenum hydroxylases like XO are widely distributed throughout nature. They have been isolated from a broad variety of organisms including bacteria, plants, birds and a wide variety of mammals like rats, cats, dogs, pigs and cows.<sup>[45]</sup> The most popular source of XO used for scientific work is by far bovine milk.<sup>[46]</sup>

### 2.2.1 Structure of xanthine oxidase

XOs from eukaryotes are large homodimers with a mass of about 290 kDa. Each of the monomers contains 4 redox active sites: a molybdenum containing active site, 2 [2Fe-2S]-clusters and FAD.<sup>[47]</sup> FAD is the prototypical cofactor of molybdenum hydroxylases.<sup>[48]</sup> Figure 8 shows a 3D image of human milk xanthine oxidase taken from the protein data base (PDB).<sup>[49]</sup>

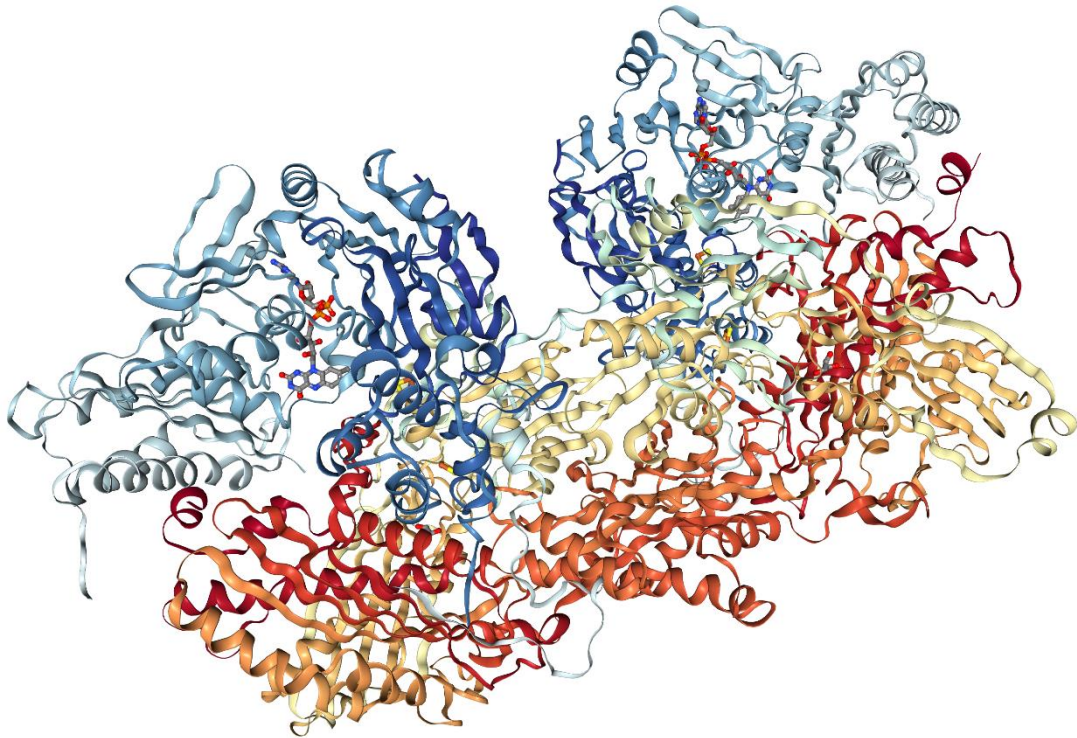
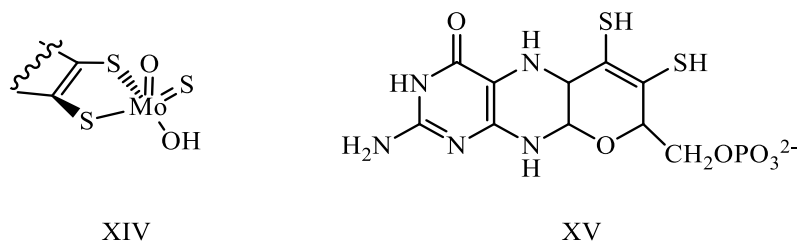


Figure 8. 3D image of human milk xanthine oxidase<sup>[49]</sup>

The overall dimensions of the dimeric enzyme are 155 Å x 90 Å x 70 Å. The two monomers form a butterfly like shape. Each of the monomer subunits can be divided into three different domains. Starting from the N-terminal end, the first domain contains the [2Fe-2S] clusters, the second domain the FAD cofactor and the larger third domain the molybdopterin-cofactor. It is sequestered in a way that puts the molybdopterin unit near the interfaces of the FAD and [2Fe-2S] domains.<sup>[50]</sup>

According to Hille<sup>[51]</sup>, the molybdenum ion in the active site is bound to 5 ligands: two sulfur atoms that link it to the pyranopterin cofactor, a double-bonded sulfur atom, a double bonded oxygen atom and a single bonded hydroxo-ligand. The structures of this molybdenum cluster and the pyranopterin cofactor can be seen in Figure 9.





**Figure 9. Structures of the molybdenum cluster in the XO active site (XIV) and the pyranopterin cofactor (XV)**

There are two possible orientations for the natural substrate to enter the active site, one where the C-8 atom is positioned in the direction of the molybdenum cluster and the other where the C-2 atom is hydroxylated.<sup>[47]</sup>

Figure 10 shows a stereoview on the active site of xanthine oxidoreductase with bound hypoxanthine. Hypoxanthine (labelled HX) is positioned in the second way described earlier.<sup>[48]</sup>

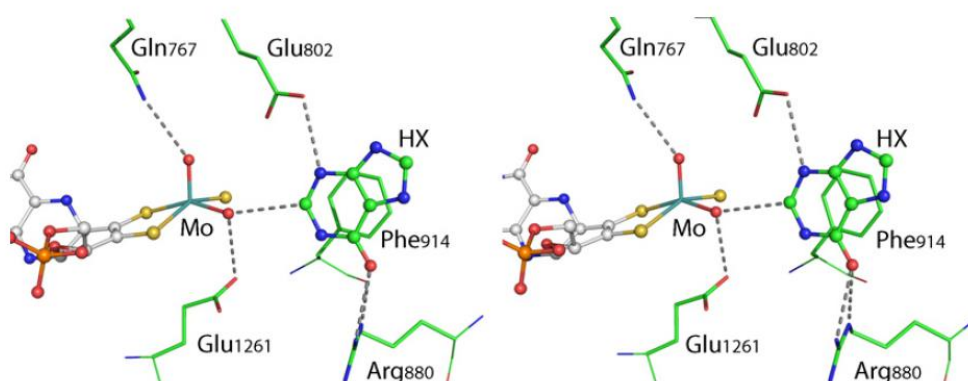


**Figure 10. Stereoview on the active site of xanthine oxidoreductase with bound hypoxanthine<sup>[48]</sup>**

As mentioned above, the two forms of the enzyme, XO and XDH, are interconvertible. The enzyme is synthesized in the XDH form and can be readily converted into the XO form. This can be done either irreversibly by proteolysis or reversibly by oxidation that leads to the formation of disulfide bridges. The main difference between the XDH and XO form is a changed reactivity of FAD towards the final electron acceptor. XO reacts rapidly with molecular oxygen, but slowly with NAD. For XDH, it's the opposite.<sup>[46]</sup>

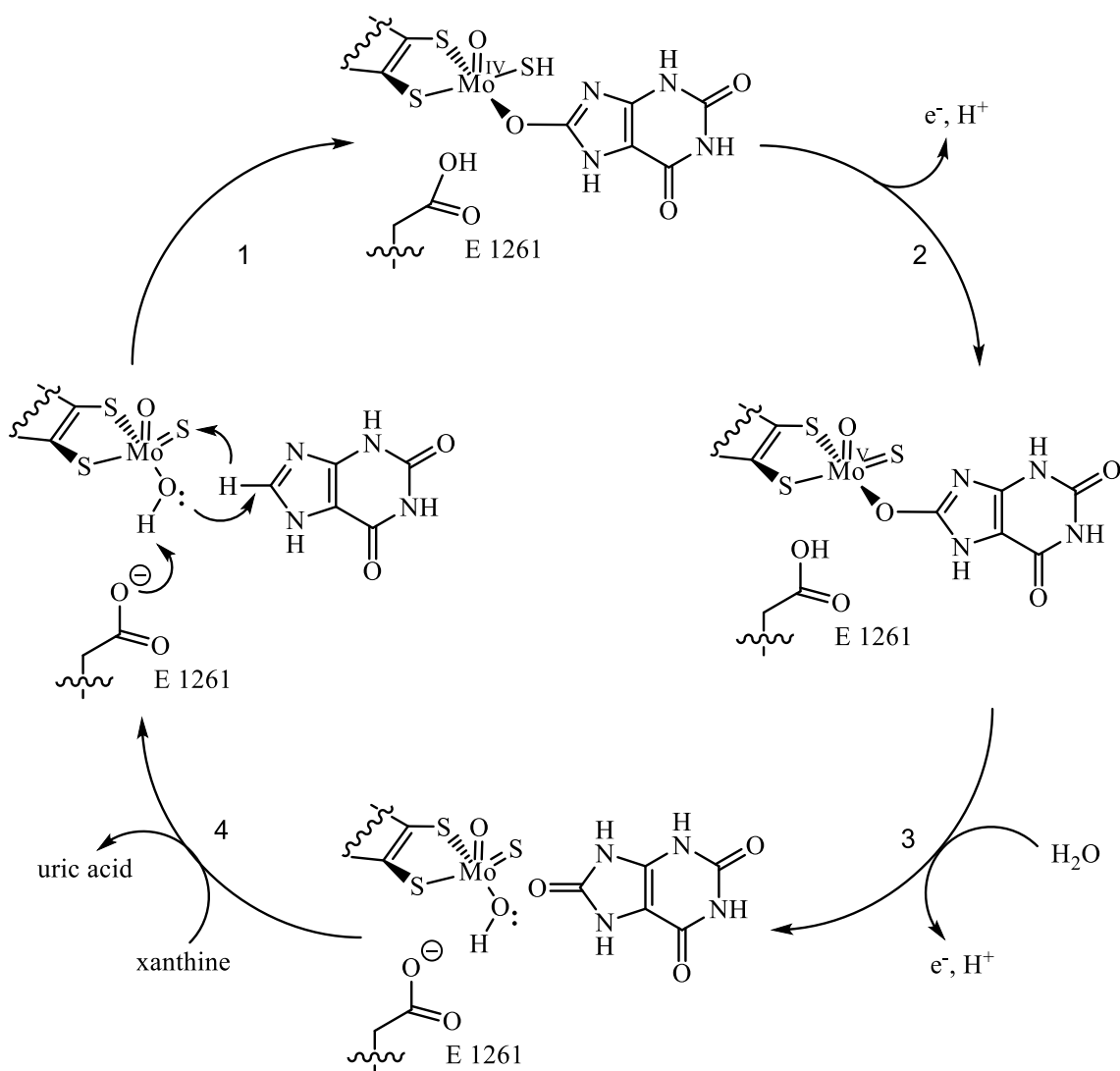
## 2.2.2 Reaction mechanism of xanthine oxidase

The enzyme number of xanthine oxidase is EC 1.17.3.2. This means it is an oxidoreductase acting on CH or CH<sub>2</sub> groups. The reaction mechanism is different from the oxidation mechanism of monooxygenases, which also catalyze hydroxylation reactions. Scheme 10 depicts the general reaction scheme of molybdenum hydroxylases.



Scheme 10. General reaction scheme of molybdenum hydroxylases

Molybdenum hydroxylases use water as the source of the hydroxyl group that is incorporated into the substrate.<sup>[48]</sup>



Scheme 11. Reaction mechanism of xanthine oxidase<sup>[47]</sup>

Scheme 11 depicts the reaction mechanism of the oxidation of xanthine to uric acid by XO as published by Cao, Puff and Hille. The catalytic cycle is started by a base assisted nucleophilic attack. E 1261 (Glu1261 in the active site model above) abstracts a proton from the hydroxo-ligand which attacks the C-atom of the substrate. Hydride transfer to the Mo=S ligand results in the reduction of the molybdenum center from Mo(VI) to Mo(IV). The molybdenum center is then re-oxidized by electron transfer to the other redox active centers of the enzyme. The Mo-SH ligand is deprotonated and the bound product is released and displaced with hydroxide from the solvent to recreate the Mo-OH ligand.<sup>[47]</sup>

### 2.2.3 Substrate scope and Inhibition of xanthine oxidase

A lot of work on the inhibition of XO is found in literature. Considerably less work has been done on the substrate scope of XO. This chapter discusses both aspects and gives examples of substrates and inhibitors of XO.

#### 2.2.3.1 Substrate scope of xanthine oxidase

Krenitsky et al.<sup>[52]</sup> tried to oxidize a variety of N-heterocyclic compounds using bovine milk XO. To enable comparison, all reaction rates of the compounds were expressed relative to the conversion of unsubstituted purine, which was set to be 100. The condensed heterocyclic core structures that showed XO activity are displayed in Figure 11, in order of decreasing reaction rates. The compounds with one oxo-substituent are included as well as the natural substrate xanthine.

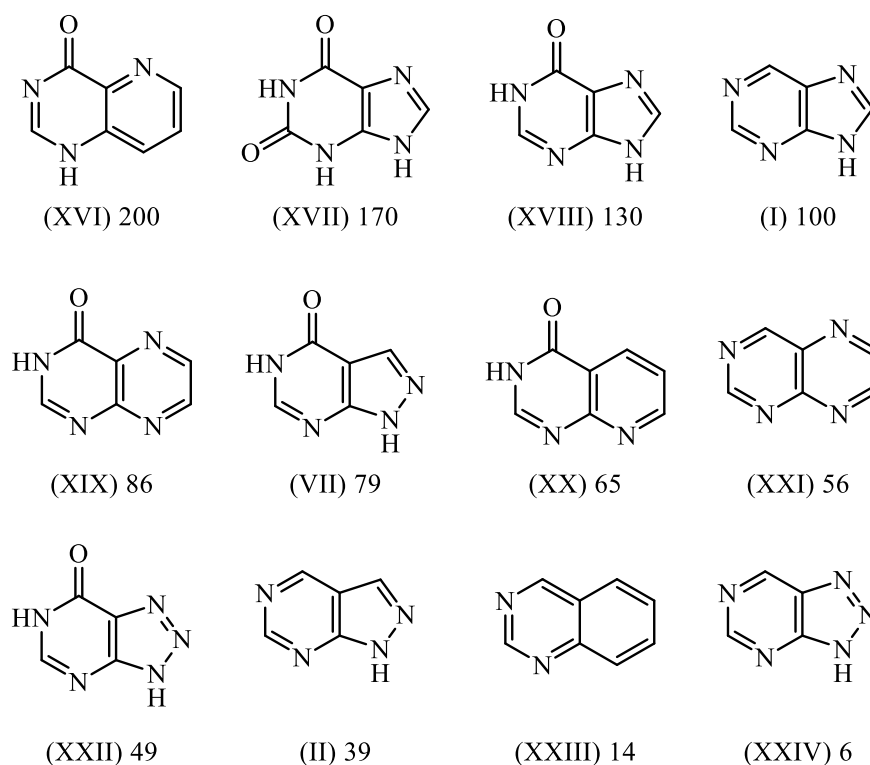


**Figure 11. Condensed heterocyclic substrates of XO with their corresponding reaction rates; (XVI) 4-oxopyrido[3,2-*d*]pyrimidine; (XVII) xanthine; (XVIII) hypoxanthine; (I) purine; (XIX) 4-oxopteridine (VII) Allopurinol; (XX) 4-oxopyrido[2,3-*d*]pyrimidine; (XXI) pteridine; (XXII) 7-oxotriazolo[4,5-*d*]pyrimidine; (II) pyrazolo[3,4-*d*]pyrimidine; (XXIII) quinazoline; (XXIV) triazolo[4,5-*d*]pyrimidine**

As can be seen in Figure 11, compounds with at least one oxo-substituent are converted faster than their unsubstituted analogs. Nearly all of the tested unsubstituted condensed pyrimidines showed XO activity. Quinoline and pyrrolo[2,3-*d*]pyrimidine were the only two unsubstituted cores that showed reaction rates lower than 3 in the work of Krenitsky. The pyrazolo[3,4-*d*]pyrimidines (**VII**) and (**II**) were found to be XO substrates and they showed that oxidation of the pyrazolo[3,4-*d*]pyrimidine scaffold in position 4 occurs prior to oxidation in position 6.

Rosemeyer and Seela<sup>[53]</sup> investigated the effects of methylation<sup>[53]</sup> in different positions of some pyrrolo[2,3-*d*]pyrimidines. They found that the purine N-7 is essential for oxidation in C-8 position. The methylation of a nitrogen in the pyrimidine moiety lowers the affinity of the substrate for XO or prevents the oxidation completely. This effect is stronger on the N-3 of the pyrrolopyrimidines than on the N-1. Furthermore, they showed that methylation on the pyrrole moiety did not have an influence on the oxidation reaction.

Another aspect of the work that was done on XO is pro-drug activation. Krenitsky et al. demonstrated the conversion of 6-deoxyacyclovir to acyclovir, a clinically used antiherpetic agent, by XO oxidation.<sup>[54]</sup> Shanmuganathan et al. reported enhanced

brain delivery of 2'-F-ara-ddI, an anti-HIV nucleoside, through oxidation of 2'-F-ara-ddP by XO.<sup>[55]</sup> Reigan et al. did work on the activation of thymidine phosphorylase inhibitors. Thymidine phosphorylase (TP) is highly expressed in many types of tumors, which makes it an interesting target for inhibition. They successfully oxidized three different types of prodrugs to form the known TP inhibitors 6A5BU, 7-DX and TPI.<sup>[56]</sup> These examples of prodrug activation are depicted in Figure 12.

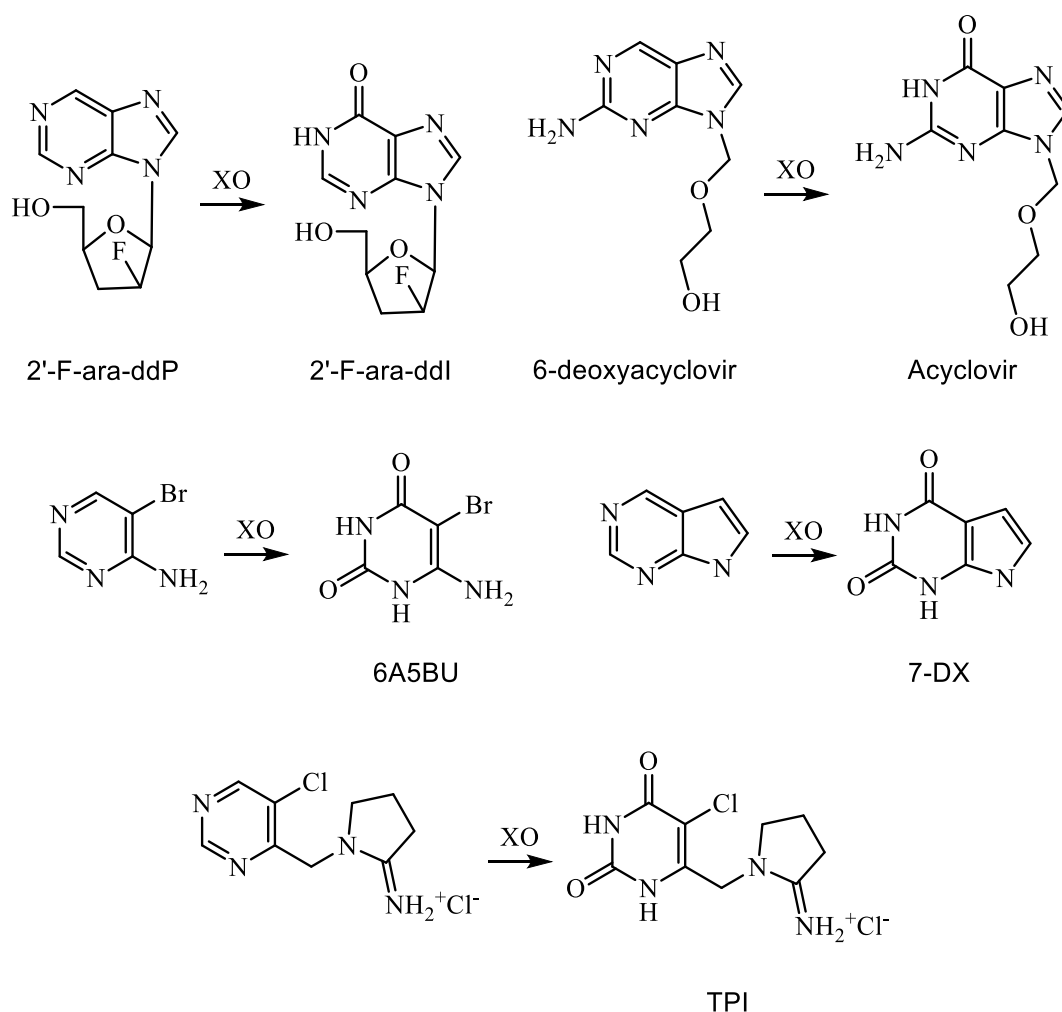


**Figure 12. Examples of prodrug activation using XO**

Reigan et al. also used the same ring systems oxidized in either position 2 or 6 of the pyrimidine ring. They also reported oxidation of the unsubstituted pyrrolo[2,3-*d*]pyrimidine, a conversion not found by Krenitsky et al.<sup>[52]</sup>, as mentioned earlier. However, they reported that it was converted at a slower rate than the oxidized analogs. It is possible that conversion occurred also in the work of Krenitsky, but at a rate that was not detected.

Lee and Han reported the oxidation of a series of imidazo[4,5-*g*]quinazolines.<sup>[57]</sup> This shows that XO is able to oxidize compounds larger than its natural substrate xanthine.

### *2.2.3.2 Inhibition of xanthine oxidase*

A lot of work on the development of XO-Inhibitors is found in the literature. Since the discovery of Allopurinol, a lot of new, more potent inhibitors of XO have been tested. This is not only due to the role of XO Inhibition in the treatment of gout, that was discussed earlier in the section on pyrazolo[3,4-*d*]pyrimidines. XO also plays a role in a lot of other diseases. High levels of uric acid play an important role in vascular diseases like hypertension, hypercholesterolemia, atherosclerosis and diabetes. Furthermore, XO generates superoxide, which is why its inhibition is beneficial in most pathophysiological states due to the reduction of oxidative stress. Therefore, XO inhibition can be beneficial in the treatment of a lot of other diseases including chronic heart failure, circulatory shock and ischemia-reperfusion (in liver, kidney, lung and other organs).<sup>[58]</sup> A complete review of XO-Inhibitors would go beyond the scope of this thesis. Therefore, Figure 13 gives examples of XO-Inhibitors found in the literature.

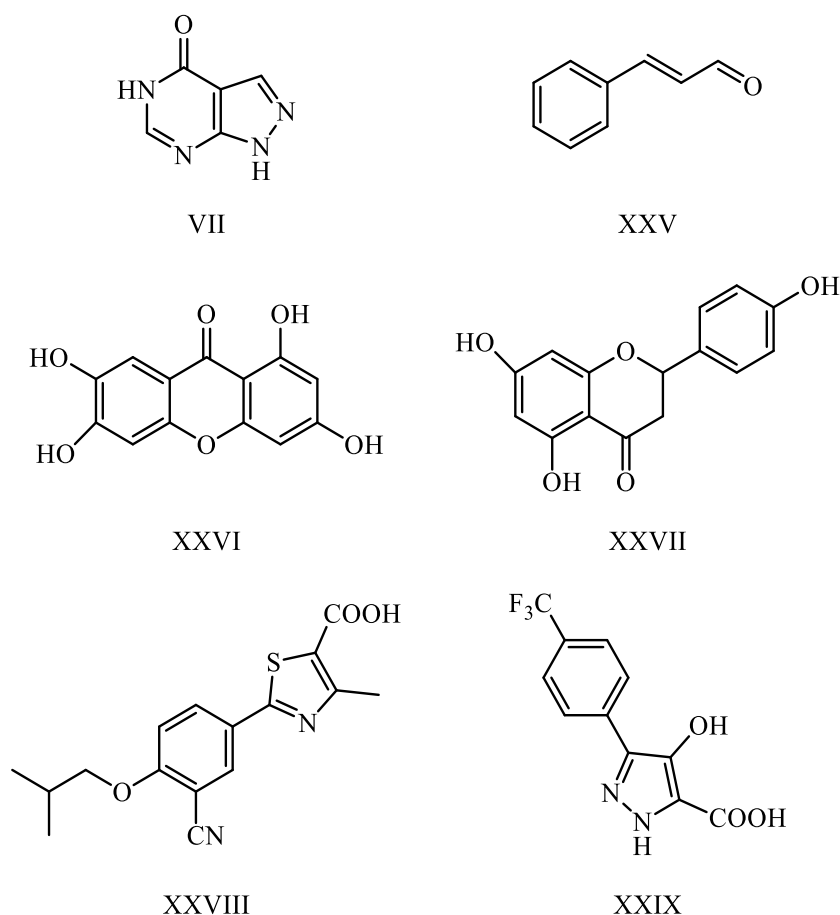


**Figure 13. (VII) Allopurinol; (XXV) cinnamaldehyde; (XXVI) norathyriol; (XXVII) Apigenin; (XXVIII) Febuxostat; (XXIX) 4-hydroxy-3-(4-(trifluoromethyl)phenyl)-1H-pyrazole-5-carboxylic acid**

These examples show the diversity of structures that have been found to effectively inhibit XO. Compounds **(XXV)**, **(XXVI)** and **(XXVII)** from Figure 13 are natural compounds. Cinnamaldehyde **(XXV)** was extracted from the essential oil from the leaves of *Cinnamomum osmophloeum*<sup>[59]</sup>, norathyriol **(XXVI)** originates from a species of fern called *Athyrium mesosorum*<sup>[60]</sup> and Apigenin **(XXVII)** is a common flavonoid from plants.<sup>[61]</sup> Norathyriol and Apigenin even surpass Allopurinol when their IC50 values are compared. (0.92  $\mu\text{M}$  and 1  $\mu\text{M}$  compared to 5.9  $\mu\text{M}$  of Allopurinol).<sup>[62]</sup>

As for examples of synthetic compounds, Febuxostat **(XXVIII)** is an interesting one. It was as effective or even surpassed Allopurinol in clinical studies on the treatment of chronic gout and it can be used for the treatment of patients with Allopurinol hypersensitivity.<sup>[63]</sup> Another example of a non-purine synthetic XO inhibitor is compound **(XXIX)** 4-hydroxy-3-(4-(trifluoromethyl)phenyl)-1H-pyrazole-5-carboxylic acid. It was assessed alongside other differently substituted pyrazole compounds by Eli Lilly and Company and was chosen as example because of the pyrazole moiety present in the compounds synthesized in this work.<sup>[64]</sup>

## 3 Results and Discussion

### 3.1 Synthesis of the targeted pyrazolo[3,4-*d*]pyrimidines

The pyrazolo[3,4-*d*]pyrimidines depicted in Figure 14 were identified as interesting targets not only for testing of oxidation by XO, but also as useful for other work conducted in this working group.

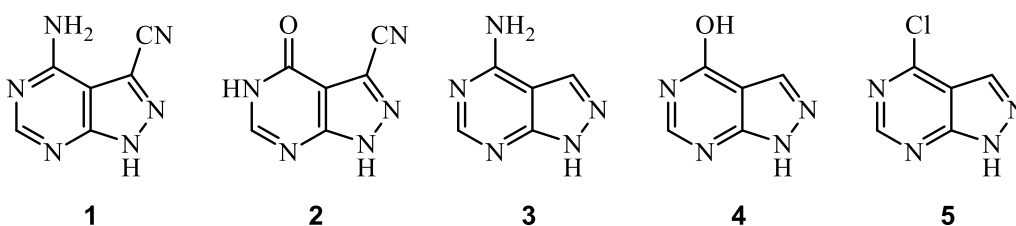
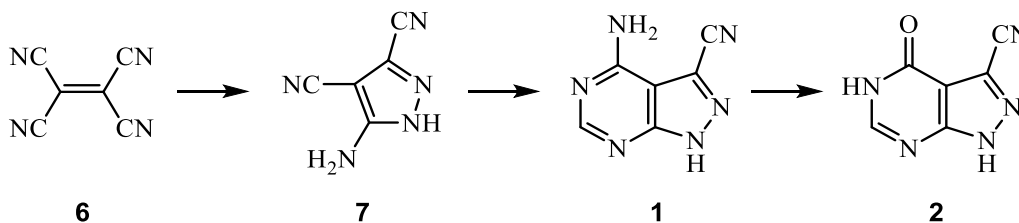


Figure 14. Targeted pyrazolo[3,4-*d*]pyrimidines

4-amino-3-cyano-1H-pyrazolo[3,4-*d*]pyrimidine (1) and 3-cyano-4-oxo-1H-pyrazolo[3,4-*d*]pyrimidine (2) were used to investigate the substrate scope of a novel enzyme, nitrile reductase queF. This enzyme is able to reduce a nitrile function to its corresponding primary amine and is part of the biosynthetic pathway to queuosine.<sup>[3]</sup>

As described earlier, there are two main strategies for the synthesis of pyrazolo[3,4-*d*]pyrimidines. The first one starting from pyrazole precursors, the second one starting from pyrimidine precursors. Functionalization of the smaller ring of the condensed ring system proved to be challenging in earlier work of this working group on pyrrolopyrimidines. Therefore it was decided to synthesize the appropriately substituted pyrazole precursors which would yield the desired substituents at the desired positions of the pyrazolo[3,4-*d*]pyrimidines. Scheme 12 depicts the proposed synthesis route to pyrazolo[3,4-*d*]pyrimidines (1) and (2).

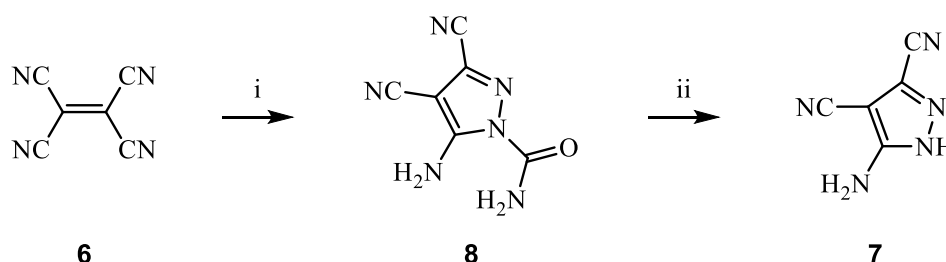


Scheme 12. Proposed synthesis route to pyrazolo[3,4-*d*]pyrimidines (1) and (2)

Following a synthesis protocol published by Dickinson et al. (Scheme 13)<sup>[65]</sup>, semicarbazide-hydrochloride was dissolved in a mixture of EtOH and triethylamine and reacted with tetracyanoethylene at 0 °C to yield 5-amino-1-carboxamido-3,4-dicyanopyrazole (8). The precipitated product was filtered from the reaction solution



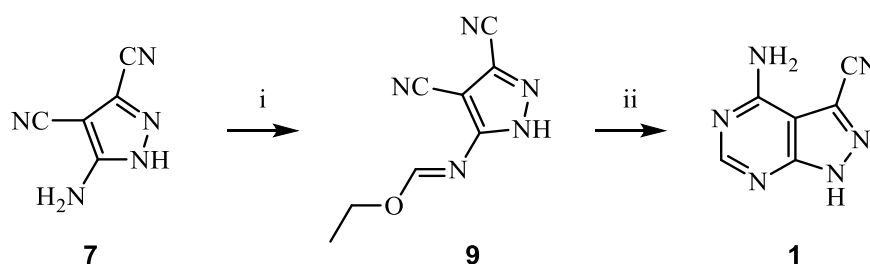
and washed with EtOH. It was subsequently added to boiling H<sub>2</sub>O dest. to give 5-amino-3,4-dicyanopyrazole (**7**) as dark red, needle like crystals that lost some of their color after recrystallization from water.



**Scheme 13. Synthesis of pyrazole precursor (**7**); (i) semicarbazide hydrochloride, EtOH, triethylamine, 0 °C; (ii) boiling H<sub>2</sub>O dest.**

The attempt to perform this two reaction steps in a one pot procedure using only H<sub>2</sub>O dest. as solvent was not successful because the removal of triethylamine during the purification made the overall procedure more complicated and resulted in a lower overall yield. Replacement of triethylamine with Na<sub>2</sub>CO<sub>3</sub> as base did not yield the desired product.

The condensation step yielding the pyrazolo[3,4-*d*]pyrimidine system proved to be the difficult part of the synthesis. Several different approaches are found in the literature and were found not to yield the desired ring system. The first approach tried was a condensation published by Taylor and Abul-Husn in 1965<sup>[12]</sup>, depicted in Scheme 14.

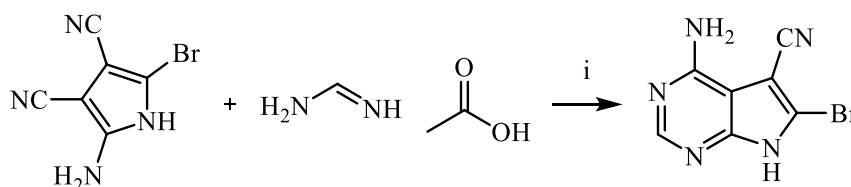


**Scheme 14. Synthesis approach to (**1**) published by Taylor and Abul-Husn; (i) triethyl orthoformate, reflux, inert atmosphere (N<sub>2</sub>), 7 h; (ii) EtOH, ethanolic ammonia (saturated at 0 °C), r.t., 24 h**

The pyrazole precursor (**7**) was reacted with triethyl orthoformate under inert atmosphere at reflux temperature for 7 h to yield the ethoxymethylamino derivative (**9**). After removal of excess triethyl orthoformate under reduced pressure, (**9**) was dissolved in 2 M ethanolic ammonia and stirred at room temperature for 24 h. The reaction did not yield the desired ring system. Therefore, 7 N methanolic ammonia from a newly opened bottle was used in a second attempt to rule out a too low concentration of ammonia in the reaction mixture. In addition, the whole reaction was performed in inert atmosphere and EtOH abs. was used to rule out the interference

of moisture as cause of reaction failure. All these measures were unsuccessful and the approach by Taylor and Abul-Husn was dismissed.

Tolman, Robins and Townsend<sup>[66]</sup> published a synthesis of a pyrrolo[2,3-*d*]pyrimidine starting from a pyrrol precursor similar to the pyrazole precursor (**7**). They used formamidine acetate in ethoxy ethanol at 140 °C to condense their precursor to the desired two ring system. Scheme 15 depicts their approach.



**Scheme 15. Pyrrolopyrimidine synthesis by Tolman et al.; (i) ethoxy ethanol, reflux, 36 h**

Since the precursor and the product only miss one nitrogen atom in a position not involved with the formation of the pyrimidine ring and the bromine substituent is not involved in the reaction, this reaction was the next approach tried to obtain pyrazolopyrimidine (**1**).

Precursor (**7**) was reacted with formamidine acetate in 2-ethoxy ethanol at reflux temperature for 54 h, since TLC analysis showed that the reaction was not completed after 36 h. Even after 54 h, the precursor had not reacted quantitatively, so the reaction was stopped to see if the desired product had formed at all. The solvent was removed under reduced pressure to yield a brown slurry. A procedure found in literature<sup>[13]</sup> for the purification of the final product of the reaction uses 50 % aq. ethanol for recrystallization. Since the reaction product did not dissolve in the aq. ethanol even when heated to 100 °C, the hot solution was filtered and HPLC analysis (Method 1) of the filtrate was performed. The chromatogram showed a peak with the *m/z* ratio of 161, the *m/z* ratio of the desired product. Therefore, the solvent was evaporated and NMR analysis of the residue was performed. NMR results did not support the claim that product was formed. If the product was formed it was in a too low concentration to give the desired peaks in NMR analysis. The reaction was repeated with more material to see if product could be isolated, but the results were the same as in the first attempt.

The next approach was to follow a synthesis protocol published by Robins et al.<sup>[5]</sup> that uses a precursor missing the cyano substituent in position 3 of the pyrazole precursor. The synthesis is depicted in Scheme 2 in the section on synthesis of pyrazolo[3,4-*d*]pyrimidines.

Formamide was mixed with CaO and stirred at 100 °C for 20 min before being distilled using reduced pressure. After distillation, the dry formamide was stored over a Union carbide type 3 Å molecular sieve. It was then added to pyrazole precursor (**7**) under inert N<sub>2</sub> atmosphere and heated to 180 °C. After a reaction time of 7.5 h, the reaction solution was cooled to 0 °C with an ice bath and H<sub>2</sub>O dest. was added to the reaction. An orange precipitate formed and was separated from the solution by filtration. The crude product was insoluble in DMSO-*d*<sub>6</sub>. The insoluble part was removed by centrifugation and the supernatant was subjected to NMR analysis. The NMR spectrum showed a lot of impurities. Therefore, the crude product was dissolved in a basic solution and re-precipitated by neutralization with acetic acid. Additionally, an activated charcoal filtration was performed. HPLC analysis (Method 2) of the product showed the formation of two compounds with *m/z* ratios of 179 and 361, but no formation of the desired product. The *m/z* ratio of 179 corresponding to a molecular weight of 178 g/mol lead to the assumption that an amide substituent in position 3 of the pyrazolo[3,4-*d*]pyrimidine system had formed.

Cataldo et al.<sup>[67]</sup> published that formamide can decompose at 185 °C to release ammonia. Ammonia could react with the cyano moiety to form an amidine, which upon hydrolysis at high temperature possibly formed the amide. The reaction was repeated at a temperature of 200 °C to see if that would lead to a different outcome. This resulted in an increase in the formation of the compound suspected to be the amide substituted ring system. The same reaction at 200 °C for 24 h resulted in a further shift towards the suspected amide. Treatment of the first reaction with NH<sub>3</sub> aq. for 3 h at 120 °C resulted in the decrease of the second byproduct and the increase of the suspected amide, which reinforced the assumption that the formation of ammonia caused this compound to form. Figure 15 shows HPLC chromatograms of the first reaction (**A**), the first reaction after treatment with NH<sub>3</sub> aq. for 3 h at 120 °C (**B**) and after 8 h at 120 °C (**C**).

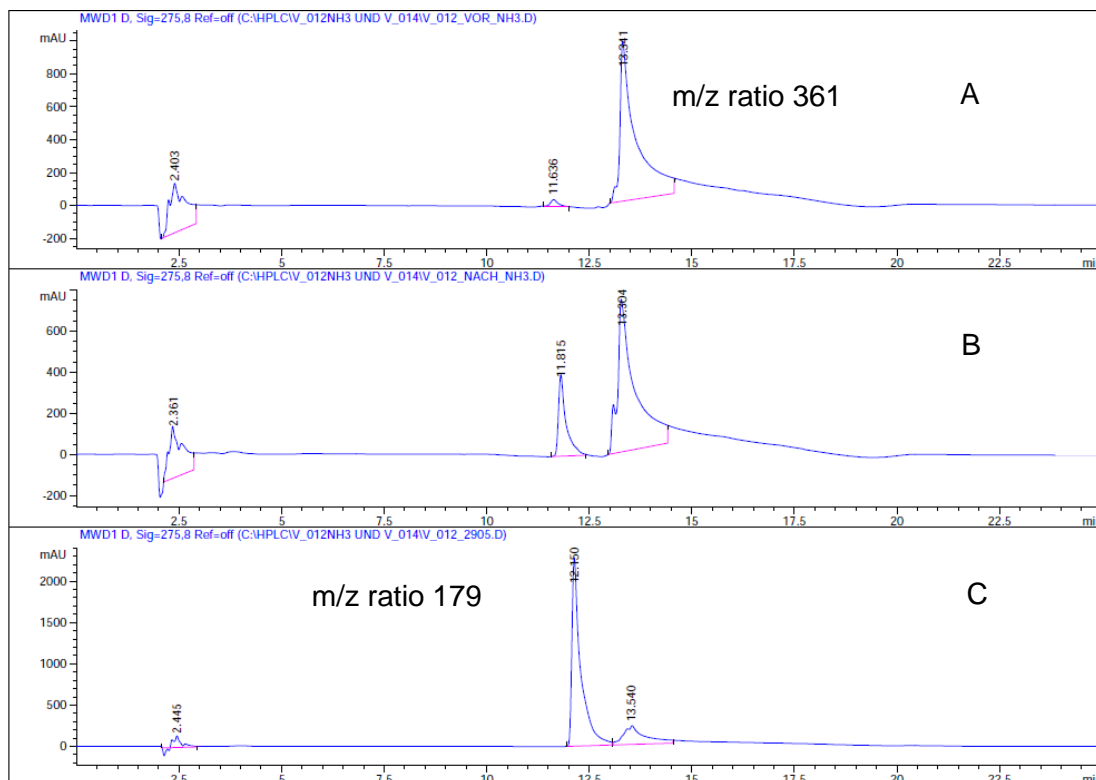
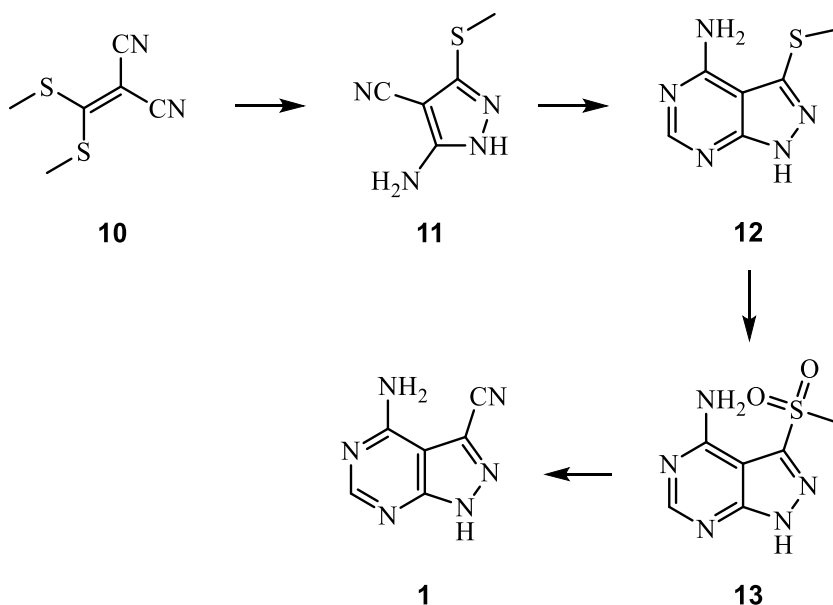


**Figure 15. HPLC chromatograms of the treatment of the condensation reaction using formamide with  $\text{NH}_3$  aq., HPLC method 2**

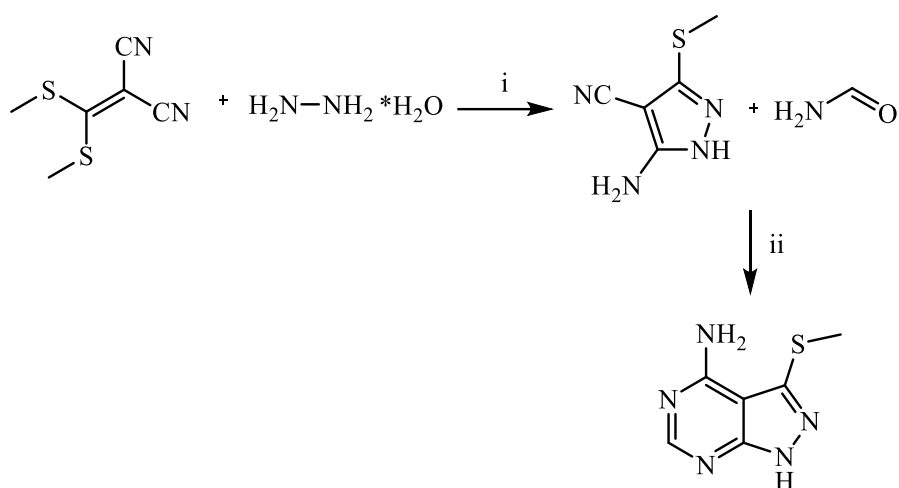
Two different methods to turn the amide into the desired cyano substituent were tried to see if the hypothesized amide formation did take place. Reactions with  $\text{Ac}_2\text{O}$  and  $\text{POCl}_3$  did not yield pyrazolopyrimidine (**1**). Therefore, the reaction with formamide was dismissed.

Another attempt to synthesize pyrazolopyrimidine (**1**) involved the exchange of a sulfone moiety in position 3 with the desired cyano substituent. Exchanges like this have been demonstrated on N-heterocycles e.g. by Martinez et al.<sup>[68]</sup> and Rankovic et al.<sup>[69]</sup>. Takahashi et al. used a sulfone-cyano exchange on a pyrazolo[1,5-a]pyridine.<sup>[70]</sup> Scheme 16 depicts the proposed synthesis route.



**Scheme 16. Proposed synthesis route to pyrazolopyrimidine (**1**) starting from 2-[Bis(methylthio)methylene]malononitrile**

Starting from 2-[Bis(methylthio)methylene]malononitrile (**10**), the pyrazole precursor (**11**) was synthesized following a synthesis protocol published by Tominaga et al.<sup>[6]</sup> (**10**) was reacted with Hydrazine-monohydrate in MeOH at reflux temperature for 2 h. The solvent was removed by evaporation and the product was recrystallized from MeOH to yield (**11**). Following the same protocol, the pyrazole precursor was reacted with formamide at reflux temperature under inert conditions. The precipitate formed after cooling with an ice bath was filtered from the reaction mixture and recrystallized from a MeOH/toluene mixture. The precipitate did not dissolve completely in hot MeOH. Therefore, the insoluble residue was separated from the solution by filtration through Celite. Addition of toluene to the filtrate and cooling yielded pyrazolopyrimidine (**12**) as an orange precipitate. Scheme 17 depicts the first two steps of this synthesis.



**Scheme 17. Synthesis of 4-amino-3-methylthiopyrazolo[3,4-d]pyrimidine; (i) MeOH, reflux temperature, 2 h; (ii) reflux temperature, 12 h**

A screening of oxidation reactions was conducted to find the best method for the oxidation of the methylthio-moiety. 50 mg of (**12**) were used in each oxidation. 6 different methods were tried, all oxidations were stirred at room temperature. Table 2 gives an overview of the used methods.

**Table 2. overview oxidation screening**

<i>variant</i>	<i>oxidizing agent</i>	<i>reaction solvent</i>
A	KMnO <sub>4</sub>	CH <sub>3</sub> COOH glacial
B	KMnO <sub>4</sub> /MnO <sub>2</sub>	DMSO
C	H <sub>2</sub> O <sub>2</sub>	CH <sub>3</sub> COOH
D	H <sub>2</sub> O <sub>2</sub>	H <sub>2</sub> O dest./isopropyl alcohol 1:1
E	NaIO <sub>4</sub>	acetone
F	Oxon/Al <sub>2</sub> O <sub>3</sub>	MeOH

All variants did oxidize the methylthio moiety. However, only variant (A) did yield the sulfone quantitatively. All other methods yielded a mixture of sulfoxide and sulfone with the majority of the product being the sulfoxide. Therefore, method (A) was used for the oxidation of the methylthiopyrazolopyrimidine (**12**). Figure 16 shows the HPLC chromatogram after the reaction for methods A and C as an example of the variants not leading to the sulfone in the applied reaction time.

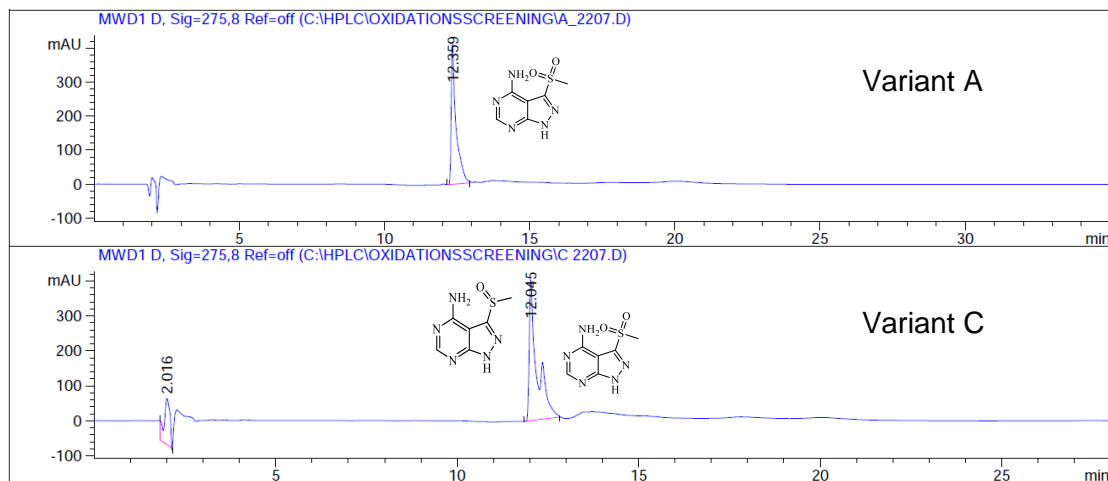


Figure 16. HPLC chromatogram after the oxidation screening, variants (A) and (C); UV signals at 275.8nm; HPLC method 2

The pyrazole precursor (**11**) was dissolved in glacial acetic acid and  $\text{KMnO}_4$  was added. The reaction mixture was neutralized after 3 h and the product was extracted from the reaction mixture with EtOAc.

The synthesized 4-amino-3-methylsulfonylpyrazolo[3,4-*d*]pyrimidine (**13**) is a new substance not yet found in the literature. It was characterized by HPLC analysis and NMR spectroscopy. Figure 17 shows the  $^{13}\text{C}$ -NMR spectrum of (**13**) with the peaks assigned to the corresponding C-atoms.

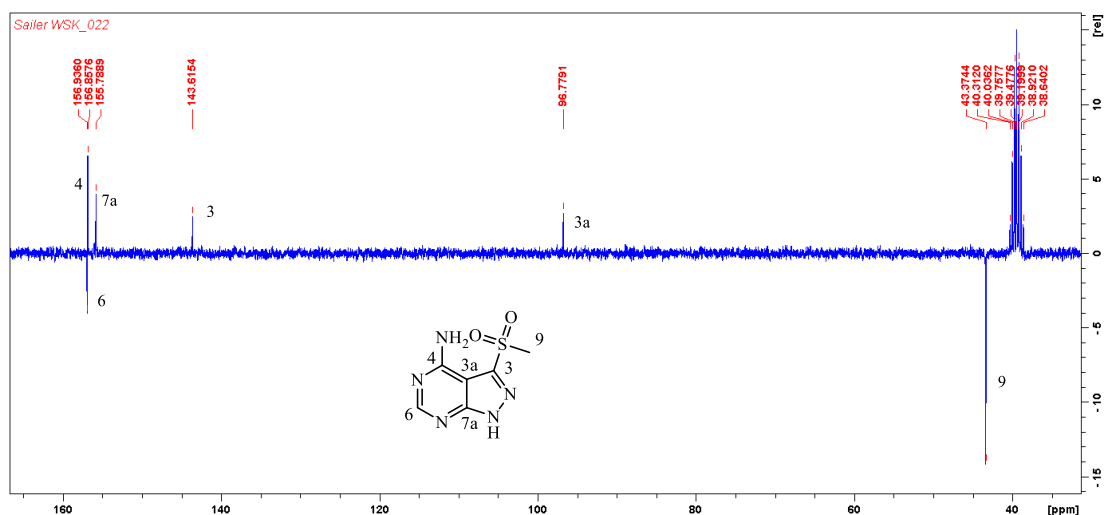


Figure 17.  $^{13}\text{C}$ -NMR spectrum of 4-amino-3-methylsulfonylpyrazolo[3,4-*d*]pyrimidine

The next step was the exchange of the methylsulfonyl moiety with the desired cyano substituent. Following the procedure used by Takahashi et al. on a pyrazolo[1,5-*a*]pyridine, the reactant was dissolved in a mixture of THF and DMF. KCN was added and the reaction mixture was heated to 80 °C. After a reaction time of 12 h, there was no conversion to the desired product. Reaction with NaCN also did not yield any product. Therefore, a higher reaction temperature of 140 °C was applied, but did not lead to the formation of the desired pyrazolopyrimidine (**1**), as was confirmed by a HPLC measurement. Figure 18 shows the chromatogram measured after the reaction.

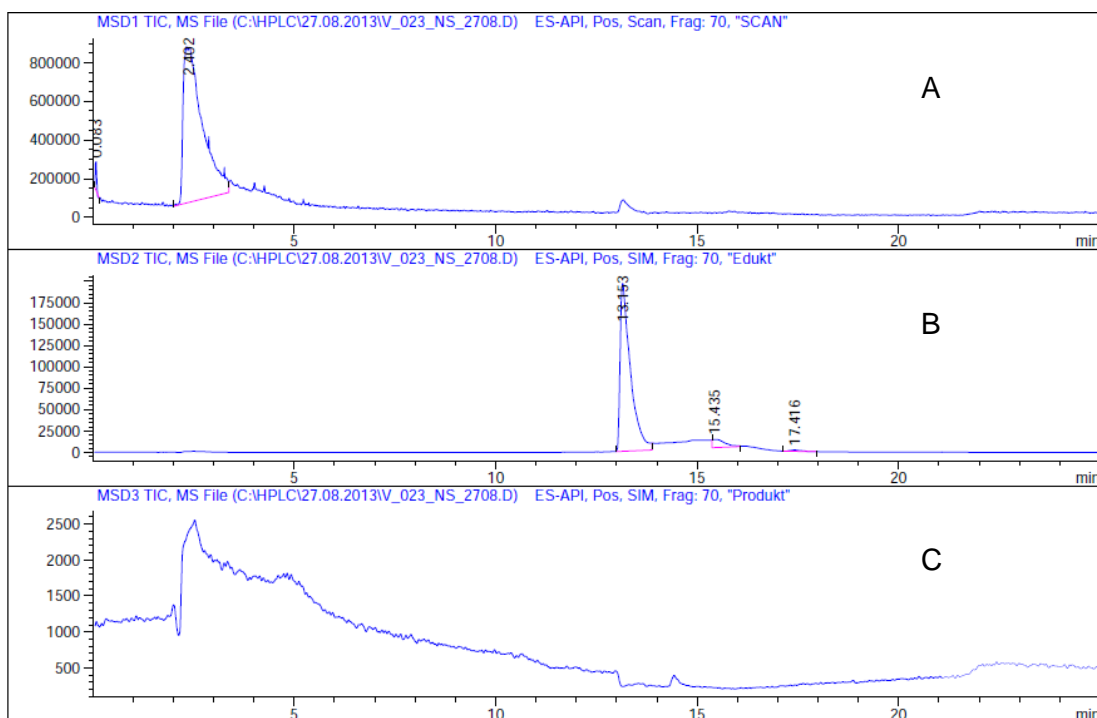
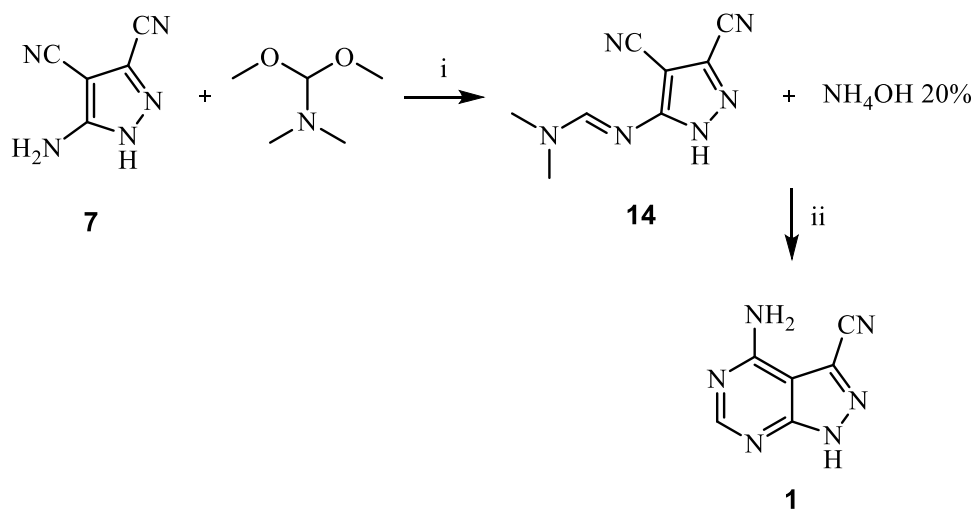


Figure 18. HPLC chromatogram of the sulfone-cyano exchange; (A) scan mode; (B) reactant (sulfone) sim; (C) product sim; HPLC method 2



The fifth approach to the synthesis of 4-amino-3-cyano-1*H*-pyrazolo[3,4-*d*]pyrimidine (**1**) was a synthesis published by Bulychev et al. in 1984<sup>[13]</sup>. It is depicted in Scheme 18.



**Scheme 18.** Bulychevs approach to pyrazolopyrimidine (**1**); (i) MeOH abs., reflux temperature; (ii) NH<sub>4</sub>OH 20 %, reflux

The first part of this synthesis is the reaction of 5-amino-3,4-dicyanopyrazole (**7**) with dimethylformamide diethylacetal to yield 3,4-dicyano-5-dimethylaminomethyleneaminopyrazole (**14**). Since dimethylformamide diethylacetal was available at the lab it was used for the reaction. The absolute MeOH used by Bulychev et al. was exchanged for DMF.

The pyrazole precursor (**7**) was dissolved in DMF and the reactant dimethylformamide diethylacetal was added. The solution was stirred at 78 °C for 1 h and 45 min. The solvent was evaporated under reduced pressure to yield (**14**). HPLC measurement proved the formation of intermediate (**14**). Figure 19 shows the chromatogram.

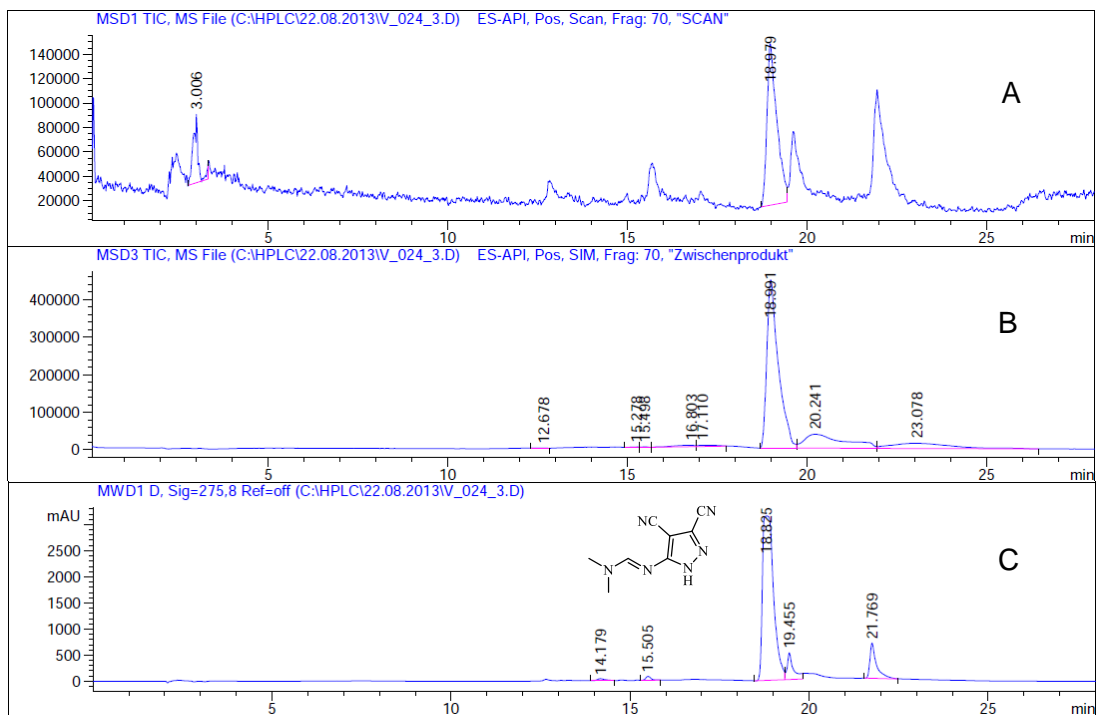


Figure 19. HPLC chromatogram of compound (14); (A) scan mode; (B) sim mode; (C) UV signal at 275.8nm; HPLC method 3

$\text{NH}_4\text{OH}$  20 % was added to the product of the first reaction step and the mixture was stirred at reflux temperature for 2 h. The product was separated from the reaction mixture by column chromatography to yield 4-amino-3-cyano-1*H*-pyrazolo[3,4-*d*]pyrimidine (**1**) as a white powder.

Figure 20 shows the  $^{13}\text{C}$ -NMR spectrum of compound (**1**) with the peaks assigned to the corresponding C-atoms.

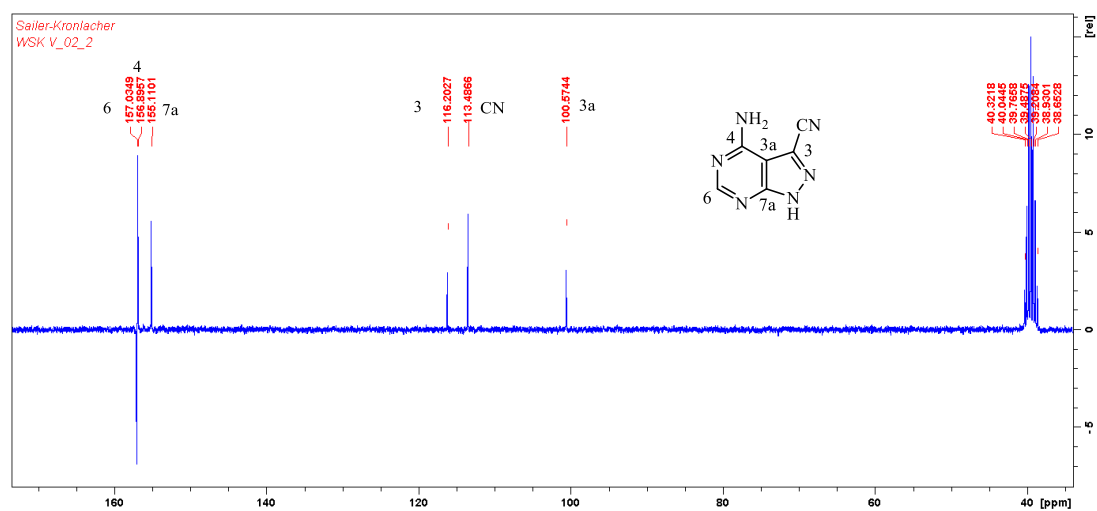


Figure 20.  $^{13}\text{C}$ -NMR spectrum of 4-amino-3-cyano-1*H*-pyrazolo[3,4-*d*]pyrimidine (**1**)

After the synthesis of pyrazolopyrimidine (**1**) was successful, the next step was a diazotization reaction according to a synthesis protocol found in literature<sup>[12]</sup> to get to the also targeted 3-cyano-4-oxo-1*H*-pyrazolo[3,4-*d*]pyrimidine (**2**). The reactant (**1**) was dissolved in HCl 8 % and stirred at 0 °C. NaNO<sub>2</sub> was dissolved in H<sub>2</sub>O dest. and added dropwise to the reaction solution over the course of 1 h. After 50 min of stirring at 0 °C, the reaction mixture was heated to 100 °C. After cooling, the reaction mixture was neutralized resulting in the precipitation of (**2**) as a white, crystalline powder. Figure 21 shows the <sup>13</sup>C-NMR spectrum of (**2**).

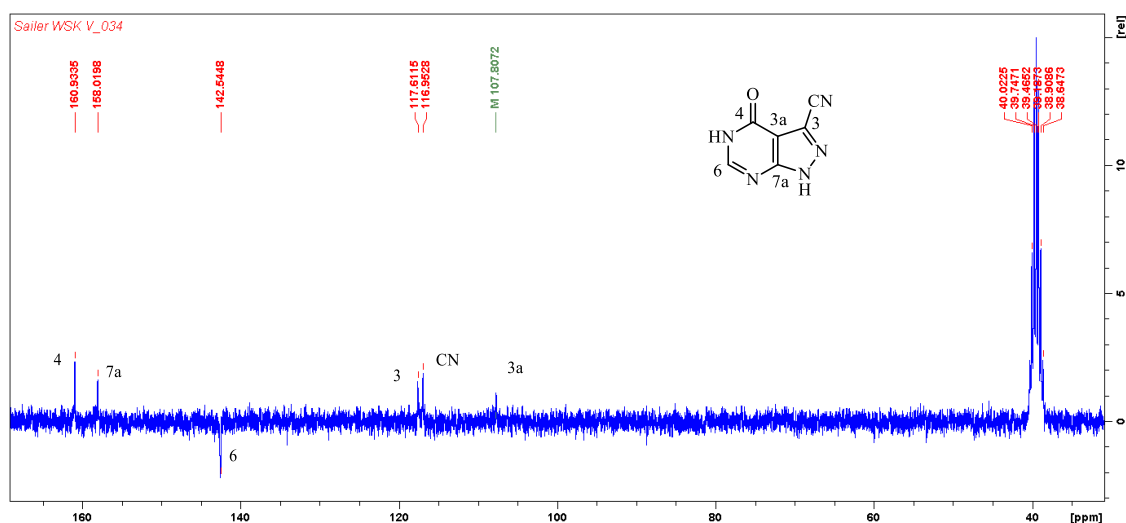
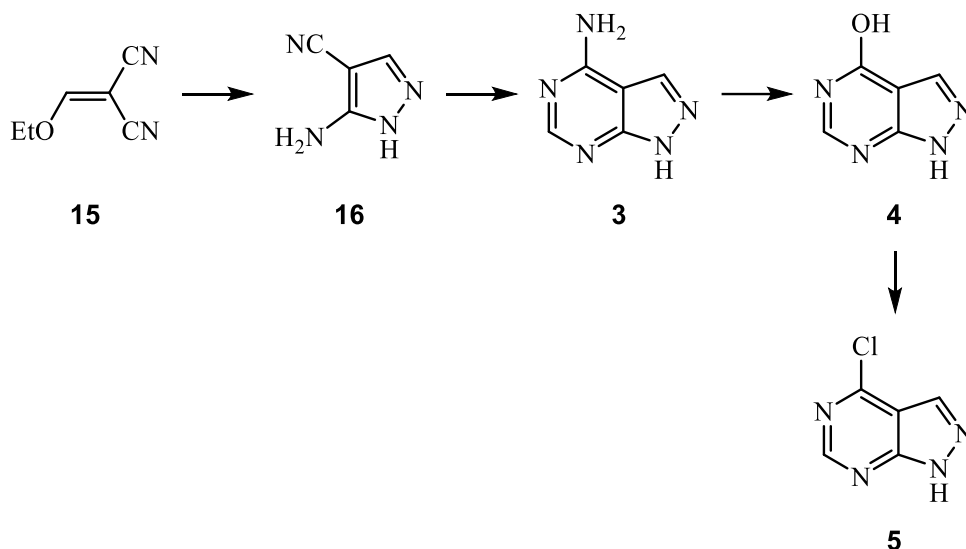


Figure 21. <sup>13</sup>C-NMR spectrum of 3-cyano-4-oxo-1*H*-pyrazolo[3,4-*d*]pyrimidine (**2**)

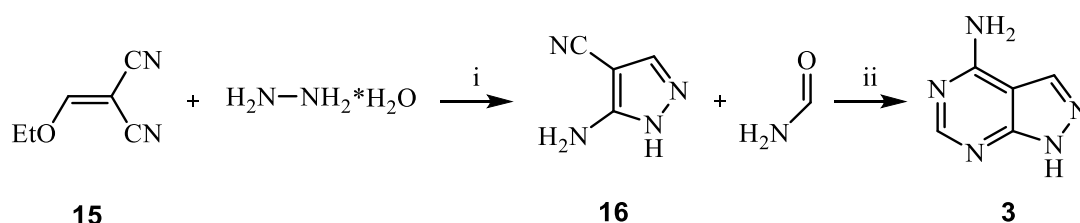
The second synthesis carried out in this work was designed to yield 4-aminopyrazolo[3,4-*d*]pyrimidine (**3**), 4-oxypyrazolo[3,4-*d*]pyrimidine (**4**, Allopurinol) and 4-chloropyrazolo[3,4-*d*]pyrimidine (**5**). The synthesis sequence is depicted in Scheme 19.



**Scheme 19. Synthesis route to targeted pyrazolopyrimidines (**3**), (**4**), and (**5**)**

The synthesis starts with the reaction of (ethoxymethylene)malononitrile (**15**) with hydrazine hydrate to form the pyrazole precursor 5-Amino-4-cyanopyrazole (**16**), as described by Robins in 1956<sup>[5]</sup>. The reactant (**15**) was dissolved in hydrazine hydrate and the mixture was heated to reflux temperature for 45 min. Cooling yielded a brown solid, which was recrystallized from H<sub>2</sub>O dest. to yield the pyrazol precursor (**16**).

The next reaction step was the condensation forming the two ring system. The reaction was carried out following a protocol by Murphy et al.<sup>[71]</sup> Scheme 20 gives a more detailed view of the first two reaction steps.



**Scheme 20. Synthesis of 4-aminopyrazolo[3,4-*d*]pyrimidine (**3**); (i) reflux temperature, 45 min; (ii) 180 °C, 8 h, inert atmosphere**

5-Amino-4-cyanopyrazole was dissolved in formamide under inert N<sub>2</sub>-atmosphere and heated to 180 °C. After 8 h of stirring at this temperature, the mixture was cooled to room temperature and H<sub>2</sub>O dest. was added resulting in the formation of an orange precipitate. The precipitate was filtered from the reaction solution and washed with

EtOAc. After drying under reduced pressure to remove formamide residues, the product of the reaction was analysed and it was confirmed that 4-aminopyrazolo[3,4-*d*]pyrimidine (**3**) had formed.

Figure 22 shows the  $^{13}\text{C}$ -NMR spectrum of (**3**).

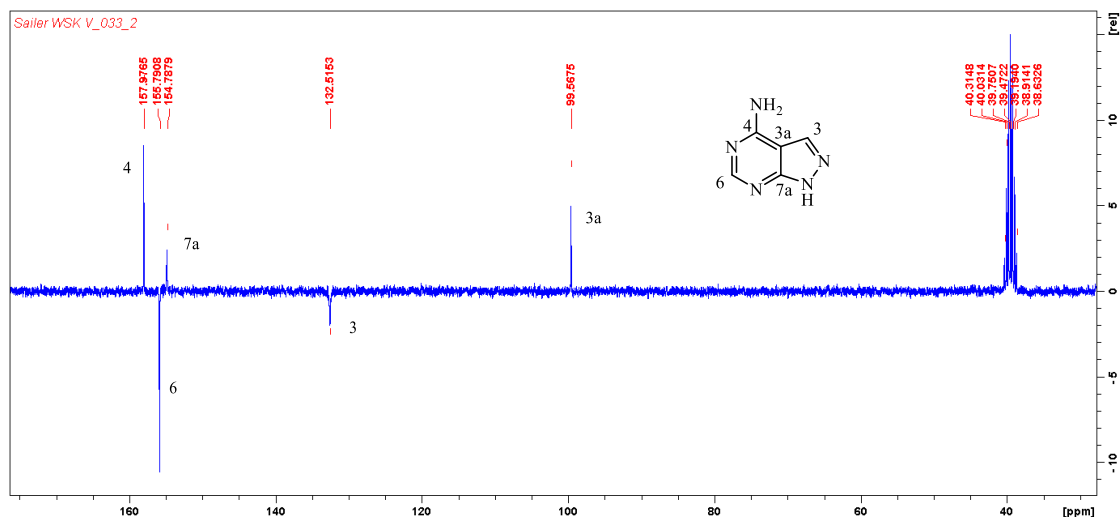


Figure 22.  $^{13}\text{C}$ -NMR spectrum of 4-aminopyrazolo[3,4-*d*]pyrimidine (**3**)

To synthesize 4-oxopyrazolo[3,4-*d*]pyrimidine (**4**), a diazotization using (**3**) as reactant was carried out. Following the same synthesis protocol used in the synthesis of (**2**)<sup>[12]</sup>, pyrazolopyrimidine (**3**) was dissolved in 8 % HCl and cooled to 0 °C.  $\text{NaNO}_2$  was dissolved in  $\text{H}_2\text{O}$  dest. and added to the solution dropwise over the course of 1h. The reaction mixture was heated to 100 °C and stirred for 5 h. Cooling lead to the formation of a precipitate, which was removed from the reaction solution by filtration and washed with acetone and recrystallized from  $\text{H}_2\text{O}$  dest.. Figure 23 shows the  $^1\text{H}$ -NMR spectrum of (**4**), Figure 24 shows the HPLC chromatogram of (**4**).

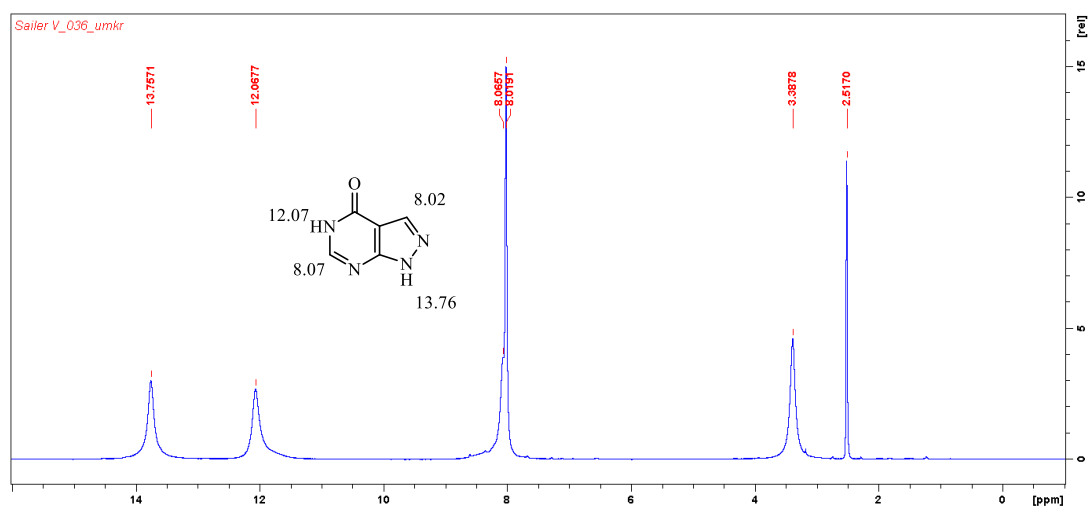
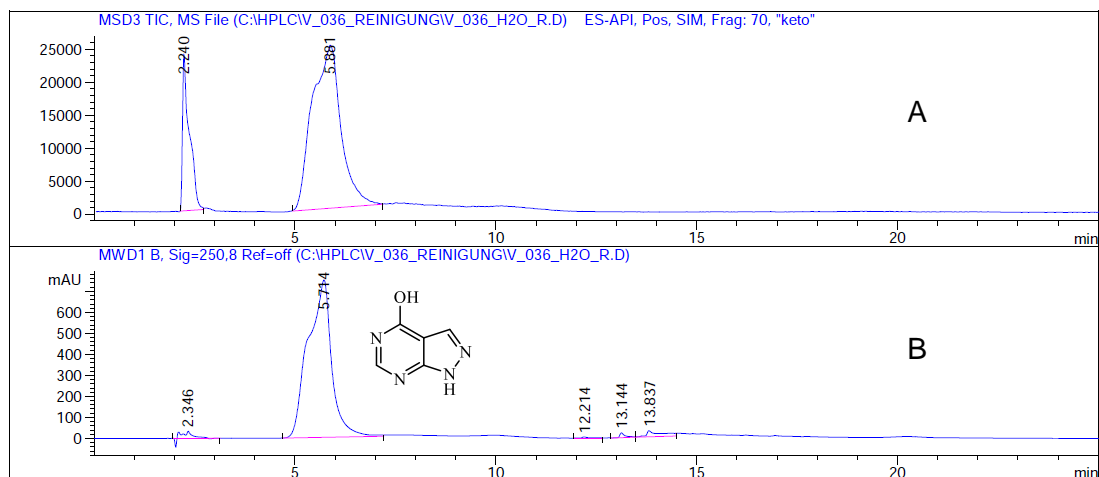


Figure 23.  $^1\text{H}$ -NMR spectrum of Allopurinol (**4**)



**Figure 24. HPLC chromatogram of Allopurinol; (A) sim mode; (B) UV signal at 250.8nm; HPLC method 4**

The final step of this synthesis was the conversion of Allopurinol (**4**) to 4-Chloropyrazolo[3,4-*d*]pyrimidine (**5**). The first attempt was an approach similar to a patent procedure published by Eli Lilly and Company in 2008.<sup>[72]</sup> They converted Allopurinol (**4**) into pyrazolopyrimidine (**5**) by reaction with phosphorus oxychloride in presence of the bulky base diisopropylethylamine. Since this base was not readily available, it was decided to use *N,N*-dimethylaniline instead.

Allopurinol (**4**) was dispersed in Toluene and POCl<sub>3</sub> and *N,N*-dimethylaniline were added. The mixture was heated to 80 °C and stirred for 6 h. The reaction was cooled to room temperature and poured into 2 M sodium phosphate dibasic. After an extraction with EtOAc and washing with cyclohexane to removed *N,N*-dimethylaniline residues, the product was analysed with HPLC-chromatography. The analysis showed the formation of the desired product (**5**) as well as the formation of a byproduct with a *m/z* ratio of 226.2. This compound was identified as 4-amino-*N*-Methyl-*N*-phenylpyrazolo[3,4-*d*]pyrimidine. Its formation arose from the contamination of the used *N,N*-dimethylaniline with *N*-methylaniline. Figure 25 shows the HPLC chromatogram.

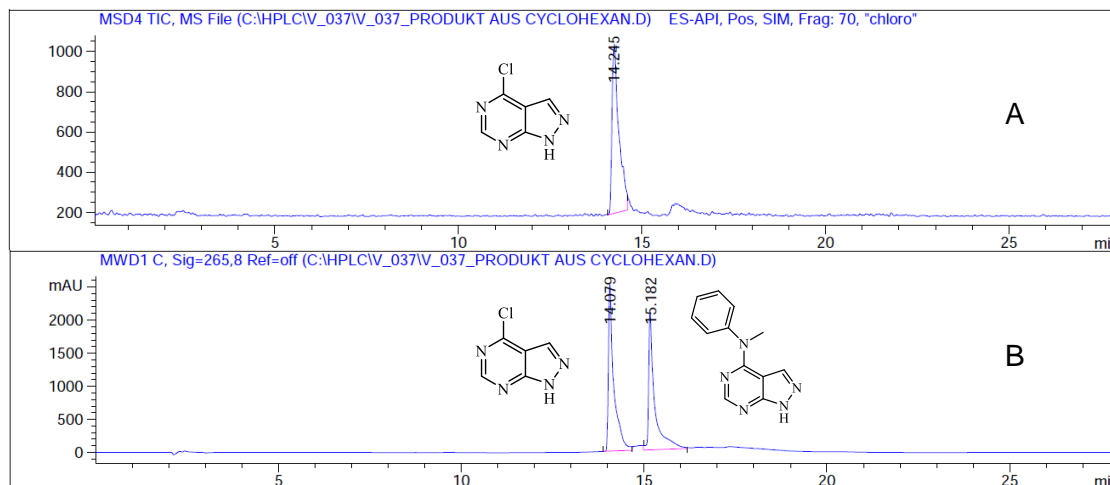


Figure 25. HPLC chromatogram of the first chlorination attempt; (A) sim mode m/z ratio compound (5); (B) UV signal 265.8nm; HPLC method 4

The next approach was to exchange the base used in the reaction. Maxwell et al. used a similar method to chlorinate pyrimidines in 2005.<sup>[73]</sup> They exchanged the base for Et<sub>3</sub>N and the solvent for ACN.

Therefore, Allopurinol (**4**) was dispersed in ACN and the other reactants were added. The reaction mixture was heated to 90 °C and stirred for 3 h. The reaction mixture was added dropwise to H<sub>2</sub>O dest. which was cooled to 0 °C and subsequently neutralized with NaOH. Extraction with Et<sub>2</sub>O yielded a mixture of the desired pyrazolopyrimidine (**5**) and a side product that was identified as 4-amino-*N,N*-diethylpyrazolo[3,4-*d*]pyrimidine. The reaction was therefore repeated with Et<sub>3</sub>N purified by a short path vacuum distillation, yielding the same product mixture as the first attempt.

The products of the two reactions that used Et<sub>3</sub>N as base were purified by column chromatography to yield 4-chloro-pyrazolo[3,4-*d*]pyrimidine as a white powder.

### 3.2 Xanthine oxidase activity test

The second part of this thesis was the development of an activity test for a specific whole cell preparation of a human xanthine oxidase (XO) expressing *E. coli* strain. Most of the work found in literature is on the inhibitory effect of a broad variety of substances on XO. This work concentrates on the ability of human XO to oxidize heterocycles other than its natural substrate Xanthine, especially on the development of a testing system with a reliable positive control. It is important that this work was done using human XO since most of the work found in the literature used XO from other sources, as was explained earlier.

The preparation of the XO expressing cells was done at ACIB (Austrian Center for Industrial Biotechnology) and was given to this working group as frozen cell pellets. Along with the cells we received the description of a basic enzymatic assay, with which the preparation of whole cells was tested. It showed high levels of XO activity. The reaction conditions of the assay are described in the following paragraph.

The whole cells were dispersed in a phosphate buffer solution (pH 7.5) and xanthine was added as 20 mM solution in 100 mM KOH to give a final concentration of 0.1 mM. The total reaction volume was 500  $\mu$ l and Eppendorf vessels were used as reaction containers. After a reaction time of 16 h at 37 °C with shaking in a thermomixer at 750 rpm, the supernatants were analyzed by HPLC/UV or HPLC/MS.

Information on the concentration of whole cell lysate (enzyme concentration) used for the test was missing. Therefore, the first enzymatic conversion was a test with the natural substrate xanthine to determine a suitable enzyme concentration for the following conversions. Three different enzyme concentrations of 1.96 g/10 ml, 1 g/ 10 ml and 0.5 g/ 10 ml were tested in combination with 3 substrate concentrations of 0.18 mM, 0.36 mM and 0.72 mM, yielding 9 combinations of enzyme and substrate concentration.

In this first attempt to find a reliable testing system for XO activity, a simple approach using thin layer chromatography was used to analyze the samples.  $\text{CHCl}_3/\text{MeOH}/\text{NH}_3$  aq. in ratio 5:4:1 was identified as a mobile phase suitable for xanthine and was therefore used for TLC reaction monitoring.



A 200 mM sodium phosphate buffer with a pH of 7.5 was used for the enzymatic conversions. The substrate was dissolved in 50 mM KOH to yield a stock solution that was added to the reaction mixture at the beginning of the reaction. The enzyme stock solution was prepared by defrosting one of the frozen pellets and dispersing 1g of the cell preparation in 5 ml of the phosphate buffer using a vortex. The rest of the pellet was refrozen immediately afterwards. The reaction solutions were prepared by adding the enzyme stock to the buffer followed by the substrate stock to yield the desired enzyme and substrate concentrations. A substrate- and an enzyme blank were used for reaction control and treated exactly the same way as the conversion samples. The reaction volume was 500  $\mu$ l, Eppendorf vessels were used as reaction containers. The vessels were then put on a thermomixer at 37 °C and 750 rpm.

The reactions were monitored by TLC using  $\text{CHCl}_3/\text{MeOH}/\text{NH}_3$  aq. in ratio 5:4:1 as mobile phase. The reaction was ended after 22.5 h reaction time. Figure 26 shows an example of a TLC chromatogram after the end of the first enzymatic conversions.

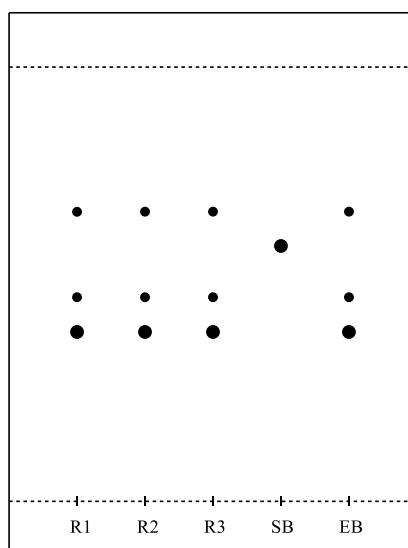


**Figure 26. TLC chromatogram of the first enzymatic conversion; (R1) c xanthine 0.72 mM, c enzyme 1.96 g/10 ml; (R2) c xanthine 0.72 mM, c enzyme 1 g/10 ml; (R3) c xanthine 0.72 mM, c enzyme 0.5 g/10 ml; (SB) substrate blank; (EB) enzyme blank**

Although no new spot appeared on the chromatograms that could be assigned to uric acid (UA), the reactions were rated to be complete due to the disappeared spot for xanthine. Therefore, all tested enzyme concentrations were suitable for the conversion.

The reactions were quenched by the addition of 100  $\mu$ l MeOH and subsequent treatment on a thermomixer at 70°C and 1400 rpm for 10 min. The samples were centrifuged and the supernatant was transferred into other vials and frozen.

Along with the natural substrate xanthine as a positive control, 5 small heterocycles of interest were the first targets for oxidation using human XO in a second batch. The targets for this second batch are depicted in Figure 27.

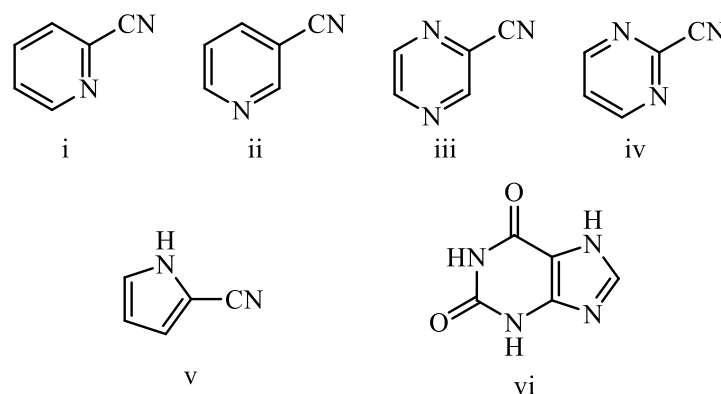


**Figure 27. possible small molecule targets for XO; (i) 2-cyanopyridine; (ii) 3-cyanopyridine; (iii) 2-cyanopyrazine; (iv) 2-cyanopyrimidine; (v) 2-cyanopyrrole; (vi) xanthine**

These targets containing a cyano moiety were chosen due to a possible further enzymatic conversion using a nitrilase to synthesize hydroxy-carboxylic acid-derivatives after the oxidation reaction. These derivatives are of interest as educts in the synthesis of various compounds. E.g. the pyrimidine derivatives are used in the synthesis of antibiotic-like compounds<sup>[74]</sup> and the pyrimidine derivatives are used as HIV-integrase inhibitors<sup>[75]</sup>.

Two different mobile phases were tested for the targeted compounds to achieve a target  $R_f$ -value of 0.7 to 0.8 for the starting compounds, because the hydroxylated products are more polar. The tested mobile phases were Toluene/MeOH/ $\text{CHCl}_3$ / $\text{Et}_3\text{N}$ / $\text{H}_2\text{O}$  in ratio 1.5:1:2:0.05:0.05 and EtOAc/EtOH/ $\text{H}_2\text{O}$ /Acetone in ratio 20:2:1:2. These mobile phases were used in this working group in work with similar compounds. The mobile phases gave similar results with  $R_f$ -values between 0.73 and 0.8 for the targeted compounds.

The conversion samples were prepared in the same matter as described for the first reaction batch, using two different enzyme concentrations of 1.96 g / 10 ml and 0.5 g / 10 ml along with a substrate blank for each compound.

The TLC chromatograms of these reactions were inconclusive. Therefore, the supernatants separated from these reactions were analyzed with HPLC/MS.

HPLC analysis was done using a reversed phase phenomenex gemini RP-18 column. HPLC methods (methods 5 and 6) were developed for the analysis of the prepared samples using gradient elution with a mobile phase combination of NH<sub>4</sub>OAc and ACN. Figure 28 shows the HPLC chromatogram of the conversion of 2-cyanopyridine. No conversion could be detected.

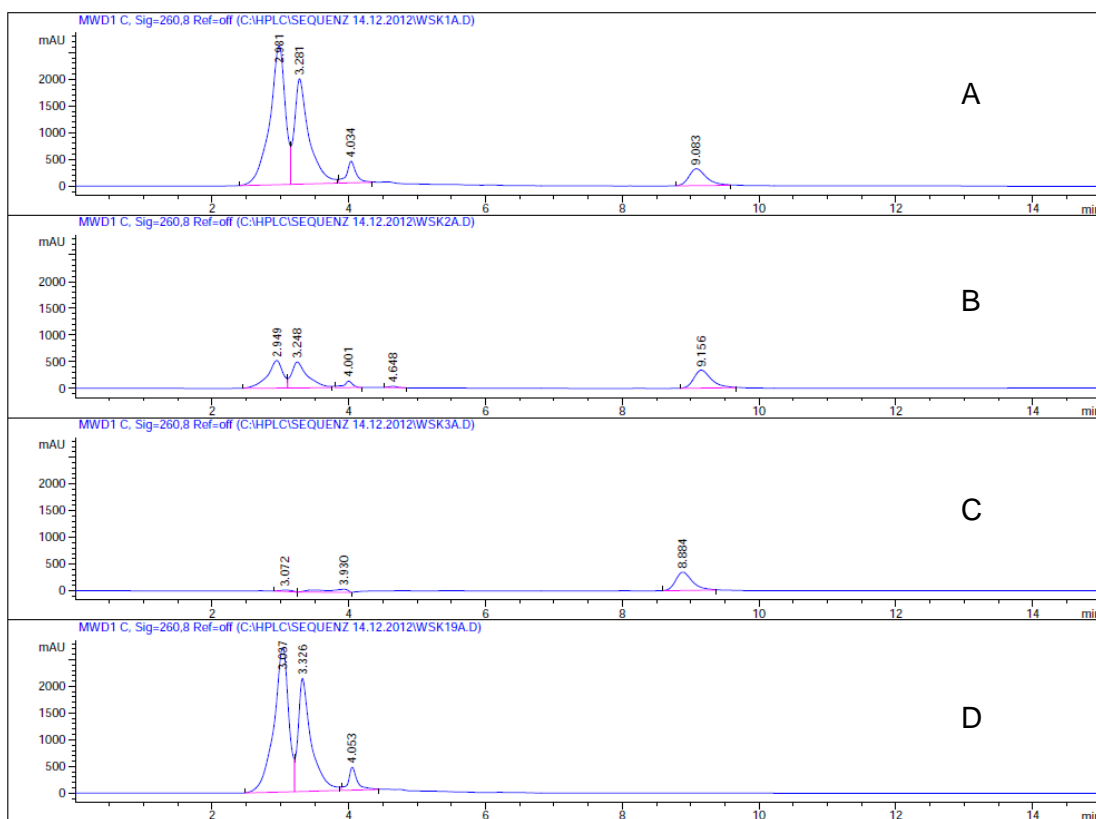


**Figure 28. HPLC chromatogram of the XO conversion of 2-cyanopyridine; (A) reaction with c enzyme 1.96 g/ 10 ml; (B) reaction with c enzyme 0.5 g/ 10 ml; (C) substrate blank; (D) enzyme blank c enzyme 1.96 g/ 10 ml; HPLC method 5**

All other conversions gave similar results, therefore a conversion using Xanthine as substrate was also analyzed with HPLC as positive control and to substantiate the claim that the conversion was successful under the applied conditions. Unfortunately, the HPLC method (method 7) used was not suitable for xanthine because of a too short retention time.

A reliable positive control for the conversions was needed. Therefore, samples of xanthine and uric acid were dissolved in KOH 50 mM and used for HPLC method development. Using gradient elution with increasing amounts of ACN, good separation was achieved for the natural substrate and the product of the enzymatic conversions. Figure 29 shows the chromatogram.

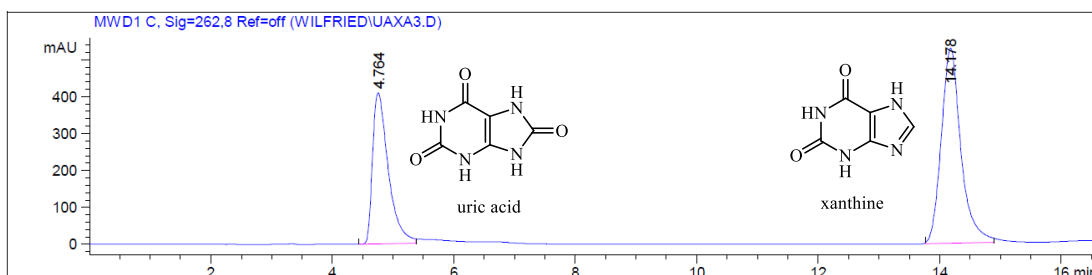


**Figure 29. HPLC chromatogram of xanthine and uric acid; UV signal at 262.8 nm; HPLC method 8**

A new reaction batch using Xanthine as substrate was set up in the way described earlier and the resulting samples were analyzed using the developed HPLC method (method 8). It was discovered that the xanthine and uric acid signals shifted to a very low retention time when dissolved in the buffer system used for the enzymatic conversions. Therefore, samples of xanthine, uric acid and enzyme stock solution in the buffer system were prepared for HPLC method development. Isocratic measurement with only 1% ACN and 99% NH<sub>4</sub>OAc resulted in the chromatogram depicted in Figure 30.

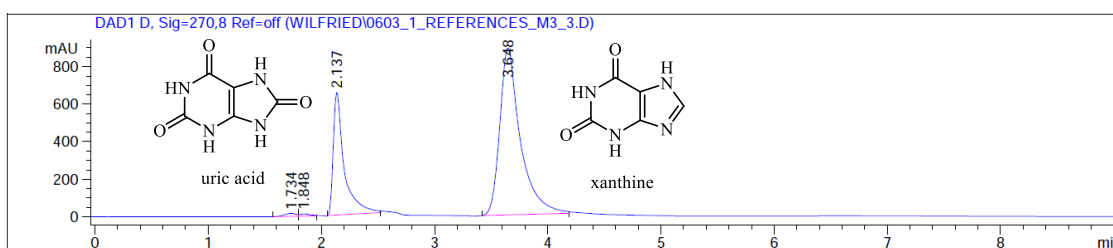


**Figure 30. HPLC chromatogram of xanthine and uric acid in the buffer system; UV signal at 270.8 nm; HPLC method 9**

This HPLC method can be used to separate xanthine and uric acid but was not suitable for a reliable positive control of XO activity. Impurities originated from the enzyme stock overlap with the peaks given by the substrate and the product peaks of the reaction.

Figure 31 shows a HPLC chromatogram of the reaction supernatant (C) along with the chromatograms of the substrate- (A) and enzyme blanks (B).

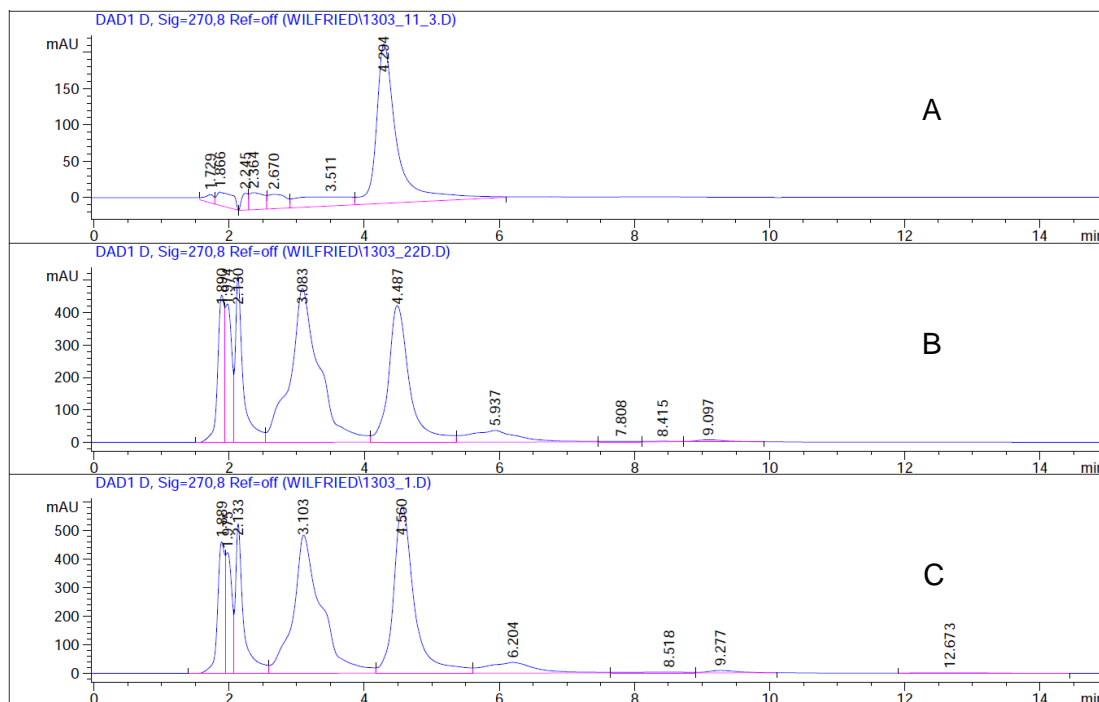
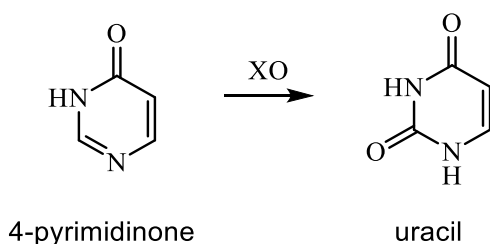


**Figure 31. HPLC chromatogram of XO conversion reaction during the development of a positive control for the activity test; (A) substrate blank; (B) enzyme blank; (C) conversion; UV signals at 270.8 nm; HPLC method 9**

As can be seen in Figure 31, this system is not suitable as a reliable positive control when the enzyme preparation is used in the way described earlier. Too many impurities are extracted from the reaction solutions and can not be separated from the natural substrate and product peaks.

Since the mobile phase used on the phenomenex gemini column could not be switched because it was in use for other projects of this working group, the next approach to get to a reliable positive control was to switch to another known substrate of XO, 4-pyrimidinone.<sup>[76]</sup> It was chosen as substrate because it was commercially available and soluble in the buffer system used. It is converted to uracil by XO. Scheme 21 depicts the conversion.



**Scheme 21. Conversion of 4-pyrimidinone by XO**

4-pyrimidinone has a too short retention time on the phenomenex gemini RP-18 column. Therefore, a LiChrospher® 100 DIOL (5  $\mu\text{m}$ ) column was examined as possible analytical system. Kazoka and Madre used a similar system to separate uracil derivatives under normal phase conditions using 4% (v/v) ethylene glycol in ethyl acetate as mobile phase<sup>[77]</sup>. H. Kazoka also used the LiChrospher® 100 DIOL column for the separation of purines and pyrimidines under normal-phase conditions in 2008.<sup>[78]</sup> The mobile phase used was water/isopropanol/hexane 3:30:67 (v/v).

The exact mobile phase could not be recreated because hexane was not available in HPLC-grade purity. It was exchanged for N-heptane and different ratios of n-heptane/isopropanol were tried during method development. Variation of column temperature was also tried. The resulting peaks for 4-pyrimidinone were too broad and tailing occurred over 5-10 min. Figure 32 gives an example of such a chromatogram.

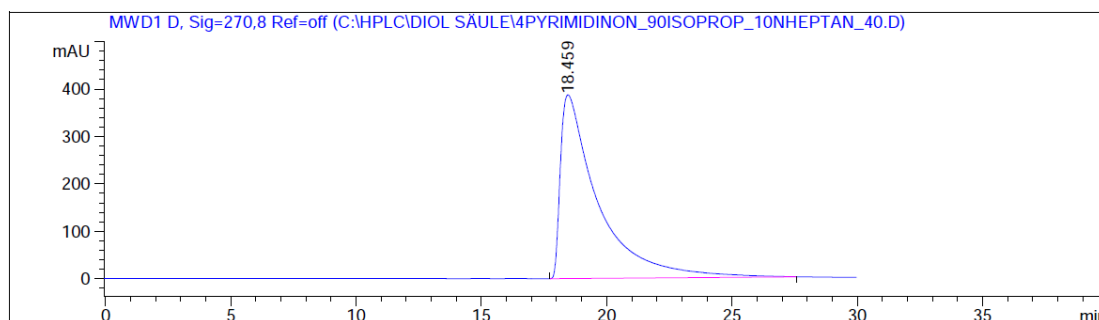


**Figure 32. HPLC chromatogram of 4-pyrimidinone on the LiChrospher® 100 DIOL column; HPLC-method 10**

The Diol column was also tested using RP-conditions. Isocratic measurement with 50% ACN and 50% NH<sub>4</sub>OAC gave good results for the separation of 4-pyrimidinone from uracil. Figure 33 shows the chromatogram.

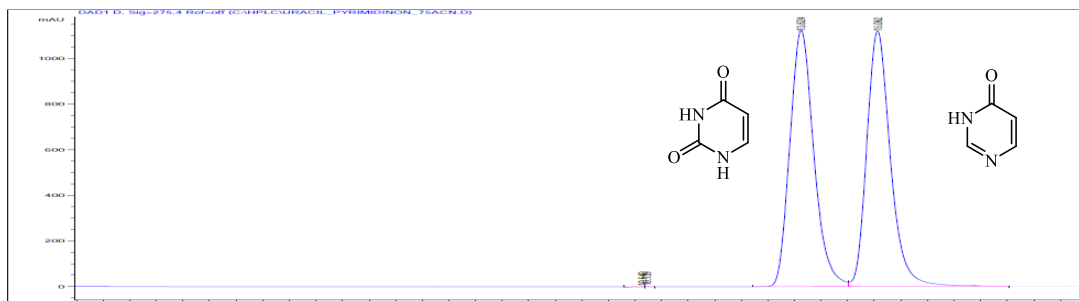


**Figure 33. HPLC chromatogram of uracil (retention time 13.62 min) and 4-pyrimidinone (retention time 15.06 min); HPLC method 11**

The biggest problem of this system is the high amount of ACN used for the analysis. This makes the system unsuitable for application it is needed for because the analysis procedure becomes too expensive.

In conclusion, the two tested columns, a phenomenex gemini RP-18 and a LiChrospher® 100 DIOL would be suitable for the 4-pyrimidinone/uracil approach for the XO activity test under the applied HPLC conditions if pure enzyme or purer enzyme preparation are available.

## 4 Conclusion and outlook

During this master thesis, the targeted pyrazolo[3,4-*d*]pyrimidines depicted in Figure 34 were successfully synthesized.

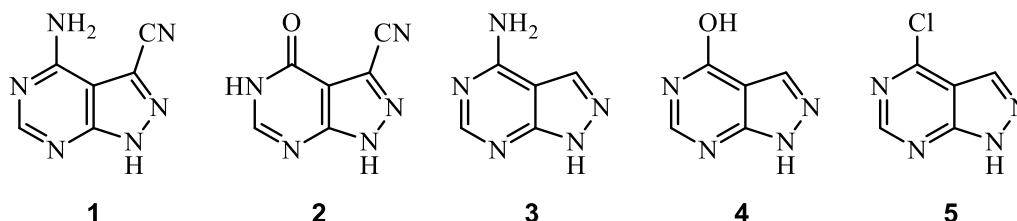


Figure 34 Synthesized targeted pyrazolo[3,4-*d*]pyrimidines

The synthesis of compounds (1) and (2) proved to be difficult but was achieved following a synthesis starting with the preparation of the appropriately functionalized pyrazole precursor. During the attempts to synthesize this two compounds, the additional two pyrazolo[3,4-*d*]pyrimidines depicted in Figure 35 were synthesized.

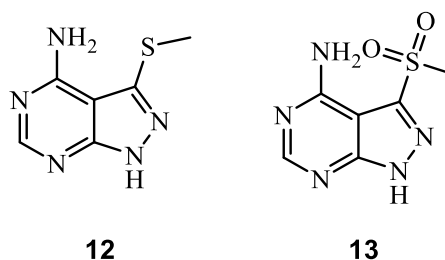


Figure 35 Pyrazolo[3,4-*d*]pyrimidines synthesized additionally to the targeted compounds

4-amino-3-(methylsulfonyl)-1*H*-pyrazolo[3,4-*d*]pyrimidine (13) is a new compound not reported in the literature up to this day.

The compounds (1) and (2) were tested in the investigation of the substrate scope of nitrile reductase queF, a novel enzyme which is able to reduce a nitrile function to its corresponding primary amine and gave promising results.

As for the xanthine oxidase activity test, the systems and conditions tested were not suited as testing system. We could not separate the natural substrate xanthine from the impurities derived from the whole cell preparation of the enzyme under the tested enzyme assay and HPLC conditions.



The two tested HPLC columns gave satisfactory results for the separation of the targeted compounds, but are not suitable as a reliable positive control of XO conversion when the whole cell lysate enzyme preparation is used. Therefore, this is the main problem that must be addressed in the future. One possible step would be to separate the enzyme from the whole cell preparation, but this would require a complex purification. If pure enzyme or a purer enzyme preparation is available, all of the tested systems are possible analytical choices for a testing system.

Continued work with the enzyme preparation used for this thesis is difficult. The peaks given by the impurities shift at rates very similar to those of the natural substrate of the enzymatic conversion. Therefore, they seem to have similar physical properties which suggests that extraction or separation will be difficult.

As for the second substrate tested as positive control, 4-pyrimidinone, the LiChrospher® 100 DIOL column has to be tested under the exact conditions given by Kazoka<sup>[78]</sup> to see if the system can be applied.

Since the buffer system used seems to be of great importance for the HPLC results, this is one point where optimization might lead to a reliable system. Other buffer systems might have a less severe influence on retention times than seen with the used sodium phosphate buffer system.

## 5 Experimental

### 5.1 General Methods

All synthesis were carried out under air unless stated otherwise. Work with air- / moisture sensitive materials was performed under inert atmosphere, using a dual vacuum/nitrogen line and standard Schlenk techniques. Flasks needed were heated under reduced pressure and ventilated with inert gas.

#### 5.1.1 Thin Layer Chromatography

Merck precoated aluminum silica gel 60 F254 plates were used for TLC. Spots were visualized by radiation with UV light at a wavelength of 254 nm. Mobile phases used were varied and are noted in the description of each synthesis.

#### 5.1.2 Column Chromatography

Merck silica gel 60 with a particle size of 63 – 200  $\mu\text{m}$  was used for column chromatography purifications. The thirtyfold to fiftyfold amount of the adsorption agent was used and light pressure was applied if necessary.

#### 5.1.3 High Performance Liquid Chromatography

HPLC analysis was carried out on an Agilent 1200 series system consisting of a G1379B Degasser, a G1312 Binary Pump SL, a G1267C High Performance Autosampler SL, a G1330 FC/ALS Thermostat, a G1316B thermostated Column Compartment SL and a G1365C Multiple Wavelength Detector SL coupled with an Agilent Technologies 6120 quadrupole LC/MS Detector with a G1918B Electrospray Ionization source.

Demineralized water was filtered through 0.2  $\mu\text{m}$  cellulose nitrate membrane filters for HPLC-buffer preparation. In most cases, a combination of ammonium acetate 20 mM buffer and acetonitrile was used as mobile phase. Gradient elution was applied as well as isocratic elution at various concentrations and mixtures. All solvents used as mobile phases were of HPLC grade purity.

The analyses were carried out using two different columns. The first column was a phenomenex Gemini-NX 3 C18 110A (150 x 2.0 mm) column, the second one a LiChrospher® 100 DIOL (5  $\mu\text{m}$ ) with LiChroCART® 250-4 guard column.

**Method 1:** Column: phenomenex Gemini; mobile phase A: ACN; mobile phase B: NH<sub>4</sub>OAc; column flow: 0.2 ml/min; column temperature: 20 °C. Stepwise gradient starting with 95% solvent B and 5% solvent A. Hold for five minutes, increase to 20% A over a period of 8 minutes, increase to 60% A over a period of 3 minutes, hold for 2 minutes, decrease to 5% A in one minute, hold for 6 minutes.

**Method 2:** Column: phenomenex Gemini; mobile phase A: ACN; mobile phase B: NH<sub>4</sub>OAc; column flow: 0.2 ml/min; column temperature: 20 °C. Stepwise gradient starting with 95% solvent B and 5% solvent A. Hold for five minutes, increase to 20% A over a period of 3 minutes, increase to 60% A over a period of 2 minutes, hold for 2 minutes, decrease to 5% A over a period of 3 minutes, hold for 10 minutes.

**Method 3:** Column: phenomenex Gemini; mobile phase A: ACN; mobile phase B: NH<sub>4</sub>OAc; column flow: 0.2 ml/min; column temperature: 20 °C. Stepwise gradient starting with 95% solvent B and 5% solvent A. Hold for five minutes, increase to 20% A over a period of 3 minutes, increase to 30% A over a period of 2 minutes, hold for 4 minutes, increase to 50% A over a period of 2 minutes, hold for 2 minutes, decrease to 5% A over a period of 1 minute, hold for 6 minutes.

**Method 4:** Column: phenomenex Gemini; mobile phase A: ACN; mobile phase B: NH<sub>4</sub>OAc; column flow: 0.2 ml/min; column temperature: 20 °C. Stepwise gradient starting with 95% solvent B and 5% solvent A. Hold for five minutes, increase to 20% A over a period of 3 minutes, increase to 40% A over a period of 2 minutes, increase to 60% A over a period of 2 minutes, hold for 2 minutes, decrease to 5% A over a period of 1 minute, hold for 10 minutes.

**Method 5:** Measurement of cyanopyridine, cyanopyrazine and cyanopyrimidine. Column: phenomenex Gemini; mobile phase A: ACN; mobile phase B: NH<sub>4</sub>OAc; column flow: 0.2 ml/min; column temperature: 20 °C. Isocratic measurement with 10% solvent A and 90% solvent B over a period of 15 minutes.

**Method 6:** Measurement of cyanopyrrole. Column: phenomenex Gemini; mobile phase A: ACN; mobile phase B: NH<sub>4</sub>OAc; column flow: 0.2 ml/min; column temperature: 20 °C. Isocratic measurement with 20% solvent A and 80% solvent B over a period of 10 minutes.

**Method 7:** Column: phenomenex Gemini; mobile phase A: ACN; mobile phase B: NH<sub>4</sub>OAc; column flow: 0.2 ml/min; column temperature: 20 °C. Stepwise gradient starting with 98% solvent B and 2% solvent A. Hold for eight

minutes, increase to 40% A over a period of 5 minutes, decrease to 2% A over a period of 2 minutes, hold for 5 minutes.

**Method 8:** Column: phenomenex Gemini; mobile phase A: ACN; mobile phase B: NH<sub>4</sub>OAc; column flow: 0.2 ml/min; column temperature: 20 °C. Stepwise gradient starting with 99% solvent B and 1% solvent A. Hold for six minutes, increase to 40% A over a period of 4 minutes, decrease to 1% A over a period of 2 minutes, hold for 10 minutes.

**Method 9:** Column: phenomenex Gemini; mobile phase A: ACN; mobile phase B: NH<sub>4</sub>OAc; column flow: 0.2 ml/min; column temperature: 20 °C. Isocratic measurement with 5% solvent A and 95% solvent B over a period of 20 minutes.

**Method 10:** Column: LiChrospher® 100 DIOL; mobile phase A: n-heptane; mobile phase B: Isopropanol; column flow 0.3 ml/min; column temperature: 40 °C. Isocratic measurement with 10% solvent A and 90% solvent B over a period of 30 minutes.

**Method 11:** Column: LiChrospher® 100 DIOL; mobile phase A: ACN; mobile phase B: NH<sub>4</sub>OAc; column flow 0.3 ml/min; column temperature: 20 °C. Isocratic measurement with 50% solvent A and 50% solvent B over a period of 20 minutes.

**Method 12:** Column: phenomenex Gemini; mobile phase A: ACN; mobile phase B: NH<sub>4</sub>OAc; column flow: 0.2 ml/min; column temperature: 20 °C. Stepwise gradient starting with 95% solvent B and 5% solvent A. Hold for five minutes, increase to 20% A over a period of 3 minutes, hold for 2 minutes, increase to 30% A over a period of 2 minutes, hold for 2 minutes, increase to 50% A over a period of 2 minutes, hold for 2 minutes, decrease to 5% A over a period of 1 minute, hold for 6 minutes.

#### 5.1.4 Nuclear Magnetic Resonance Spectroscopy

<sup>1</sup>H-NMR and <sup>13</sup>C-NMR were recorded on a Bruker AVANCE III spectrometer with autosampler (<sup>1</sup>H-NMR: 300.36 MHz, <sup>13</sup>C-NMR: 75.53 MHz). Chemical shifts for <sup>1</sup>H-NMR are reported in ppm related to Me<sub>4</sub>Si as internal standard. Signal multiplicities were assigned with the subsequent abbreviations: s (singlet), br s (broad singlet), d (doublet), br d (broad doublet), dd (doublet of a doublet), t (triplet), q (quadruplet) and m (multiplet). Depending on the solubility of the substances, deuterated

dimethyl sulfoxide (DMSO-*d*6) or deuterated chloroform (CDCl<sub>3</sub>) were used as solvents.

### 5.1.5 Biotransformations

#### **Phosphate-buffer preparation:**

Buffers were prepared fresh before each experiment. 5.76 g of Na<sub>2</sub>HPO<sub>4</sub> and 1.12 g of NaH<sub>2</sub>PO<sub>4</sub> were dissolved in 250 ml H<sub>2</sub>O dest. to yield a 200 mM pH 7.5 sodium phosphate buffer.

#### **Whole cell enzyme preparation:**

The preparation of the XO expressing cells was done at ACIB (Austrian Center for Industrial Biotechnology) and was given to this working group as frozen cell pellets.

Samples were taken either by cracking up a frozen pellet and weighing or by defrosting a pellet and sampling the then slimy whole cell preparation and refreezing immediately afterwards.

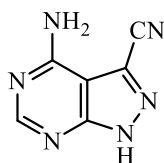
The cells were then dispersed in the phosphate buffer by rotation of a spatula or vortexing to yield the enzyme stock solution.

#### **Enzymatic conversions:**

Substrates were dissolved in 50 mM KOH. The reaction solutions were prepared by adding the enzyme stock to the buffer followed by the substrate stock to yield the desired enzyme and substrate concentrations. The reaction volume was 500 µl, Eppendorf vessels were used as reaction containers. The vessels were then put on a thermomixer at 37 °C and 750 rpm with opened covers to ensure sufficient O<sub>2</sub> supply. The reactions were quenched by the addition of 100 µl MeOH and subsequent treatment on a thermomixer at 70°C and 1400 rpm for 10 min. The samples were centrifuged and the supernatant was transferred into other vials and frozen.

## 5.2 Synthesis of pyrazolo[3,4-*d*]pyrimidines

### 4-amino-3-cyano-1*H*-pyrazolo[3,4-*d*]pyrimidine (1)



4-amino-3-cyano-1*H*-pyrazolo[3,4-*d*]pyrimidine was prepared according to a modified literature procedure.<sup>[13]</sup>

DMF (4ml) and dimethylformamide dimethylacetal (2.8 ml, 19.4 mmol) were added to 5-amino-3,4-dicyanopyrazole (2.35 g, 17.6 mmol) and the resulting mixture was heated to 80 °C. DMF (12 ml) was added in portions of 2 ml until all solids were dissolved. The reaction mixture was stirred at 80 °C for 1 h and 40 min. The solvent was evaporated in vacuum afterwards. The resulting solid (3.38 g) was dissolved in NH<sub>4</sub>OH 20% (25 ml) and the mixture was heated to 100 °C for 2 h, then cooled to 0 °C and neutralized with HCl. The neutralized solution was stored in a fridge overnight. The resulting precipitate was collected by filtration and washed with cold H<sub>2</sub>O dest. The filtrate was reduced to half under vacuum and cooled with an ice bath to give another batch of precipitate. The combined precipitates were dried in vacuum and the product was purified by silica gel column chromatography (CH<sub>2</sub>Cl<sub>2</sub>/MeOH 20:1). White solid (0.43 g, 15 % yield).

TLC: CH<sub>2</sub>Cl<sub>2</sub>/MeOH 10:1; R<sub>f</sub>: 0.29

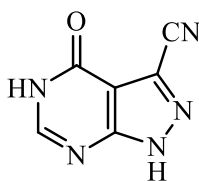
<sup>1</sup>H-NMR (DMSO-*d*<sub>6</sub>): δ 7.61 (bs, 2H, NH<sub>2</sub>), 8.3 (s, 1H, H-6), 14.68 (bs, 1H, NH)

<sup>13</sup>C-NMR (DMSO-*d*<sub>6</sub>): δ 100.57 (C-3a), 113.49 (CN), 116.2 (C-3), 155.11 (C-7a),  
156.9 (C-4), 157.03 (C-6)

The NMR data is in accordance to literature.<sup>[79]</sup>

HPLC-MS, method 12; retention time: 13.372 min

### 3-cyano-4-hydroxy-1*H*-pyrazolo[3,4-*d*]pyrimidine (2)



3-cyano-4-hydroxy-1*H*-pyrazolo[3,4-*d*]pyrimidine was prepared according to a modified literature procedure.<sup>[12]</sup>

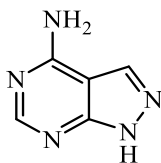
A suspension of 4-amino-3-cyano-1*H*-pyrazolo[3,4-*d*]pyrimidine (0.22 g, 1.4 mmol) in HCl 8% (4 ml) was stirred at 0 °C. NaNO<sub>2</sub> (0.95 g, 14 mmol) was dissolved in 3.5 ml H<sub>2</sub>O dest. and added dropwise to the reaction mixture over the course of 1 h. Additional NaNO<sub>2</sub> (0.19 g, 2.7 mmol) was dissolved in H<sub>2</sub>O dest. and added to the reaction mixture. HCl 8% (1 ml) was added and the mixture was stirred for another 50 min at 0 °C. Subsequently, the reaction was heated to 100 °C, stirred for 10 min and then cooled to 0 °C again. The product was precipitated from the reaction mixture by neutralizing the solution with aqueous sodium hydroxide (2M). The precipitate was isolated by filtration and washed with cold H<sub>2</sub>O dest. and by cold acetone. The white precipitate was dried in vacuum to yield 0.10 g (yield 45%) of the desired product.

TLC: CHCl<sub>3</sub>/MeOH/NH<sub>3</sub> aq. 5:4:1; R<sub>f</sub>: 0.67

<sup>1</sup>H-NMR (DMSO-*d*<sub>6</sub>): δ 7.68 (s, 1H, H-6), 7.86 (bs, 1H, H-5), 11.39 (bs, 1H, H-1)

<sup>13</sup>C-NMR (DMSO-*d*<sub>6</sub>): δ 107.72 (C-3a), 116.95 (C-3), 117.61 (CN), 142.54 (C-6),  
158.02 (C-7a), 160.93 (C-4)

### 4-amino-1*H*-pyrazolo[3,4-*d*]pyrimidine (3)



4-amino-1*H*-pyrazolo[3,4-*d*]pyrimidine was prepared according to a modified literature procedure.<sup>[71]</sup>

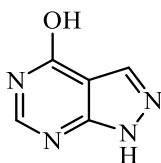
Formamide (22.5 ml, 560 mmol) was added to 5-amino-4-cyano-1*H*-pyrazole (4.596 g, 42 mmol) under nitrogen atmosphere. The mixture was heated to 180 °C for 8 h, cooled and stored in a fridge overnight. Cold H<sub>2</sub>O dest. (10 ml) was added, the precipitate was collected by filtration and washed with H<sub>2</sub>O dest. and EtOAc. The resulting solid was dried in vacuum to yield 4-amino-1*H*-pyrazolo[3,4-*d*]pyrimidine (5.0688 g, 90.11 % yield).

TLC: CH<sub>2</sub>Cl<sub>2</sub>/MeOH 5:1; R<sub>f</sub>: 0.35

<sup>1</sup>H-NMR (DMSO-*d*<sub>6</sub>): δ 7.62 (bs, 2H, NH<sub>2</sub>), 8.09 (s, 1H, H-6), 8.15 (s, 1H, H-3),  
13.35 (bs, 1H, H-1)

<sup>13</sup>C-NMR (DMSO-*d*<sub>6</sub>): δ 99.57 (C-3a), 132.52 (C-3), 154.79 (C-7a), 155.79 (C-6),  
157.98 (C-4)

### 4-hydroxy-1*H*-pyrazolo[3,4-*d*]pyrimidine (4) / Allopurinol



4-hydroxy-1*H*-pyrazolo[3,4-*d*]pyrimidine was prepared according to a modified literature procedure.<sup>[12]</sup>

HCl (90 ml) was added to 4-aminopyrazolo[3,4-*d*]pyrimidine (4 g, 29.6 mmol) at 0 °C. NaNO<sub>2</sub> (20.44 g, 296 mmol) was dissolved in H<sub>2</sub>O dest. (35 ml) and the resulting solution was added dropwise to the reaction mixture in the course of 1 h. The pH-value was checked and another 10 ml of HCl were added to keep the reaction mixture strongly acidic. Another batch of NaNO<sub>2</sub> (4.12 g, 59.7 mmol) dissolved in 15 ml H<sub>2</sub>O dest. was added to the reaction mixture in portions. The reaction mixture was stirred



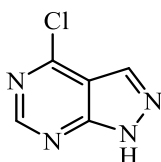
at 0 °C for 2 h and afterwards heated to 100 °C. Another 2 g of NaNO<sub>2</sub> were added and the reaction was cooled to r.t. after 3h and stirred overnight. The resulting mixture was cooled to 0 °C and the formed precipitate was collected by filtration and washed with H<sub>2</sub>O dest. and acetone. Yield: 76%

TLC: CH<sub>2</sub>Cl<sub>2</sub>/MeOH 10:1; R<sub>f</sub>: 0.25

<sup>1</sup>H-NMR (DMSO-d<sub>6</sub>): δ 8.02 (s, 1H, H-3), 8.07 (s, 1H, H-6), 12.07 (bs, 1H, H-4), 13.76 (bs, 1H, H-1)

HPLC-MS, method 4; retention time: 5.881 min

#### 4-chloro-1*H*-pyrazolo[3,4-*d*]pyrimidine (5)



4-chloro-1*H*-pyrazolo[3,4-*d*]pyrimidine was prepared according to a modified literature procedure.<sup>[73]</sup>

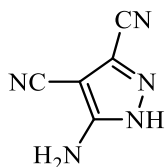
1 ml Et<sub>3</sub>N was added to a suspension of 0.5 g (3.6 mmol) Allopurinol in 5 ml ACN. 0.72 ml (7.7 mmol) of POCl<sub>3</sub> were added dropwise and the resulting mixture was heated to 90 °C to yield an orange solution. The reaction was stirred for 3h and cooled to room temperature afterwards. H<sub>2</sub>O dest was cooled to 4 °C and added dropwise to the reaction. The resulting strongly acidic solution was neutralized with NaOH 2M and the product was extracted with Et<sub>2</sub>O. This yielded a mixture of the desired product with 4-diethylamino-1*H*-pyrazolo[3,4-*d*]pyrimidine. The reaction was repeated twice, once without ACN as solvent and once with distilled Et<sub>3</sub>N. All 3 attempts gave the same product mixture. The second attempt was done with 0.5 g of Allopurinol, the third with 2.02 g. The reactions were combined and the final product was isolated with silica gel column chromatography (CH<sub>2</sub>Cl<sub>2</sub>/MeOH 80:1). White powder, overall yield 15%.

TLC: CH<sub>2</sub>Cl<sub>2</sub>/MeOH 10:1; R<sub>f</sub>: 0.7

<sup>13</sup>C-NMR (DMSO-d<sub>6</sub>): δ 112.46 (C-3a), 132.78 (C-3), 153.38 (C-7a), 154.48 (C-6), 154.57 (C-4)

HPLC-MS, method 4; retention time: 13.799 min

### 5-amino-3,4-dicyano-1*H*-pyrazole (7)



5-amino-3,4-dicyano-1*H*-pyrazole was prepared according to a modified literature procedure.<sup>[65]</sup>

Semicarbazide hydrochloride (8.71 g, 78.1 mmol) and triethylamine (10.9 ml, 78.1 mmol) were added to 200 ml of ethanol and stirred for 1 h to yield a light yellow suspension. The suspension was cooled on an ice bath and tetracyanoethylene (10.02 g, 78.1 mmol) was added in portions. The reaction mixture was stirred for 4 h and 30 min at 0 °C. Subsequently, the yellow reaction mixture was boiled for 30 min and the produced gas was captured in two successive traps of aqueous sodium hydroxide (5M). The reaction mixture was cooled to 0 °C and the formed precipitate was collected by filtration and washed with cold ethanol. The precipitate was added to boiling water in portions resulting in strong gas formation and foaming. The reaction mixture was refluxed for 1 h, then cooled and stored in a fridge overnight. The formed precipitate was collected by filtration, the filtrate was reduced to half in vacuum and cooled in the fridge to give another batch of product which was isolated by filtration. This was repeated two more times and the precipitates were combined and dried in vacuum to yield 6.28 g (60 % yield) of light red needle shaped crystals.

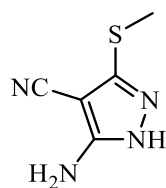
TLC: CH<sub>2</sub>Cl<sub>2</sub>/MeOH 10:1; R<sub>f</sub>: 0.36

<sup>1</sup>H-NMR (DMSO-d<sub>6</sub>): δ 7.04 (s, 2H, NH<sub>2</sub>), 13.17 (s, 1H, NH)

<sup>13</sup>C-NMR (DMSO-d<sub>6</sub>): δ 75.24 (C-4), 112.41 (CN), 112.56 (CN), 125.19 (C-3),  
153.28 (C-5)

The NMR data is in accordance to literature.<sup>[80]</sup>

### 5-amino-4-cyano-3-(methylthio)-1*H*-pyrazole (11)



5-amino-4-cyano-3-(methylthio)-1*H*-pyrazole was prepared according to a modified literature procedure.<sup>[6]</sup>

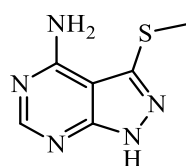
2-[Bis(methylthio)methylene]-malononitrile (5 g, 29.4 mmol) was dispersed in MeOH (100 ml). A hydrazine monohydrate solution (3.5 ml, 50% w/w N<sub>2</sub>H<sub>4</sub>, 35.2 mmol) was added and the reaction mixture was boiled at reflux temperature for 2 h. The reaction was cooled to room temperature and a fine black precipitate was removed by filtration. The solvent was removed in vacuum and the resulting solid was recrystallized from MeOH to give the desired product (3.91 g, 86.3 % yield)

TLC: Toluene/MeOH/CHCl<sub>3</sub>/Et<sub>3</sub>N/H<sub>2</sub>O dest. 1.5:1:2:0.05:0.05; R<sub>f</sub>: 0.43

<sup>1</sup>H-NMR (DMSO-*d*<sub>6</sub>): δ 11.21 (bs, 1H, NH), 6.39 (s, 2H, NH<sub>2</sub>), 2.43 (s, 3H, CH<sub>3</sub>).

<sup>13</sup>C-NMR (DMSO-*d*<sub>6</sub>): δ 154.04 (C-5), 146.79 (C-3), 114.29 (CN), 72.26 (C-4), 13.52 (-CH<sub>3</sub>).

### 4-amino-3-(methylthio)-1*H*-pyrazolo[3,4-*d*]pyrimidine (12)



4-amino-3-(methylthio)-1*H*-pyrazolo[3,4-*d*]pyrimidine was prepared according to a modified literature procedure.<sup>[6]</sup>

4 ml formamide were added to 3.8 g (24.6 mmol) of 5-amino-4-cyano-3-(methylthio)-1*H*-pyrazole and heated to 180 °C under stirring. After 3 h reaction time, TLC analysis showed that the reaction was not complete. Therefore, 2 ml of formamide were added and the reaction was stirred at 150 °C over night. After 10 h at that temperature, the reaction was heated to 180 °C again and stirred at that temperature for another 10 h. TLC analysis showed no more changes. Therefore the reaction was cooled with an ice bath and the formed precipitate was

filtered from the solution and washed with H<sub>2</sub>O dest.. The precipitate was recrystallized from MeOH/Toluol to give 4-amino-3-(methylthio)-1*H*-pyrazolo[3,4-*d*]pyrimidine. Yield 75%.

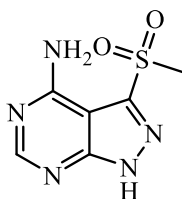
TLC: CH<sub>2</sub>Cl<sub>2</sub>/MeOH 10:1; R<sub>f</sub>: 0.35

<sup>1</sup>H-NMR (DMSO-*d*<sub>6</sub>): δ 13.39 (bs, 1H, NH), 8.16 (s, 1H, H-6), 7.18 (bs, 2H, NH<sub>2</sub>), 2.58 (s, 3H, CH<sub>3</sub>)

<sup>13</sup>C-NMR (DMSO-*d*<sub>6</sub>): δ 157.59 (C-4), 156.19 (C-6), 156.03 (C-7a), 139.07 (C-3), 98.77 (C-3a), 15.50 (CH<sub>3</sub>)

HPLC-MS, method 2; retention time: 13.4 min

#### 4-amino-3-(methylsulfonyl)-1*H*-pyrazolo[3,4-*d*]pyrimidine (13)



4-amino-3-(methylthio)-1*H*-pyrazolo[3,4-*d*]pyrimidine (3.12 g, 17.22 mmol) was dissolved in 280 ml glacial CH<sub>3</sub>COOH. KMnO<sub>4</sub> (9.53 g, 60 mmol) was added in portions under stirring to yield a violet solution. The reaction was stirred at room temperature for 3.5 h and then neutralized with MeOH and Na<sub>2</sub>CO<sub>3</sub>. This resulted in the formation of a large amount of salt. Extraction with EtOAc and subsequent solvent evaporation under reduced pressure yielded 0.53 g of the desired product (15% yield). The low yield is due to the not optimal treatment after the reaction. The reaction was not repeated because enough product for the testing of the next reaction step was derived from the first attempt.

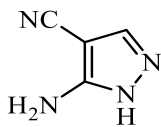
TLC: EtOH/EE/Et<sub>2</sub>O 1:1:1; R<sub>f</sub>: 0.75

<sup>1</sup>H-NMR (DMSO-*d*<sub>6</sub>): δ 8.34 (s, 1H, H-6), 8.24 (bs, 1H, NH), 7.24 (bs, 2H, NH<sub>2</sub>), 3.49 (s, 3H, CH<sub>3</sub>)

<sup>13</sup>C-NMR (DMSO-*d*<sub>6</sub>): δ 156.94 (C-4), 156.86 (C-6), 155.79 (C-7a), 143.61 (C-3), 96.78 (C-3a), 43.37 (CH<sub>3</sub>)

HPLC-MS, method 2; retention time: 12.522 min

### 5-amino-4-cyano-1*H*-pyrazole (16)



5-amino-4-cyano-1*H*-pyrazole was prepared according to a modified literature procedure.<sup>[5]</sup>

(Ethoxymethylene)malononitrile (10 g, 81.9 mmol) was added to hydrazine hydrate (8 ml, 128.4 mmol) in portions under stirring. After half of the addition, the reaction mixture was cooled to 0 °C. Another batch of hydrazine hydrate (1 ml, 16.05 mmol) was added to dissolve the formed solid mass. The reaction mixture was heated to reflux for 45 min and then cooled to room temperature to give a solid mass again. H<sub>2</sub>O dest. (5 ml) was added and the reaction mixture was treated with an ultrasonic bath for 10 seconds. The resulting mixture was filtered and the precipitate was washed with cold H<sub>2</sub>O dest.. The solid precipitate was recrystallized twice from H<sub>2</sub>O dest. to yield the desired product (5.04 g, 57% Yield), which was used for the next reaction step without further purification.

TLC: CH<sub>2</sub>Cl<sub>2</sub>/MeOH 10:1; R<sub>f</sub>: 0.4

## 6 References

- [1] Schenone, S.; Radi, M.; Musumeci, F.; Brullo, C.; Botta, M. *Chem. Rev.* **2014**, *114*, 7189–7238.
- [2] Kitamura, S.; Sugihara, K.; Ohta, S. *Drug Metab. Pharmacokinet.* **2006**, *21*, 83–98.
- [3] Van Lanen, S. G.; Reader, J. S.; Swairjo, M. A.; de Crécy-Lagard, V.; Lee, B.; Iwata-Reuyl, D. *Proc. Natl. Acad. Sci. U. S. A.* **2005**, *102*, 4264–4269.
- [4] Moss, G. P. *Pure Appl. Chem.* **1998**, *70*, 143–216.
- [5] Robins, R. K. *J. Am. Chem. Soc.* **1956**, *78*, 784–790.
- [6] Tominaga, Y.; Honkawa, Y.; Hara, M.; Hosomi, A. *J. Heterocycl. Chem.* **1990**, *27*, 775–783.
- [7] Southwick, P.L.; Dhawan, B. *J. Heterocycl. Chem.* **1975**, *12*, 1199–1205.
- [8] Taylor, E. C.; Patel, M. *J. Heterocycl. Chem.* **1991**, *28*, 1857–1861.
- [9] Warmhoff, H.; Ertas, M. *Synthesis (Stuttg.)* **1985**, *2*, 190–194.
- [10] Quinn, R. J.; Scammells, P. J. *Tetrahedron Lett.* **1991**, *32*, 6787–6788.
- [11] Taylor, E. C.; Hartke, K. S. *J. Am. Chem. Soc.* **1959**, *81*, 2456–2464.
- [12] Taylor, E. C.; Abul-Husn, A. *J. Org. Chem.* **1965**, *31*, 342–343.
- [13] Bulychev, Y. N.; Korbukh, I. A.; Preobrazhenskaya, M. N.; Chernyshov, A. I.; Esipov, S. E. *Chem. Heterocycl. Compd.* **1984**, *20*, 215–221.
- [14] Cheng, C. C.; Robins, R. K. *J. Org. Chem.* **1958**, *23*, 191–200.
- [15] Inoue, S.; Nagano, H.; Nodiff, E. A.; Saggiomo, A. J. *J. Med. Chem.* **1964**, *7*, 816–818.
- [16] Taylor, E. C.; Borrer, A. L. *J. Org. Chem.* **1961**, *26*, 4967–4974.
- [17] Oliveira-Campos, A. M. F.; Sivasubramanian, A.; Rodrigues, L. M.; Seijas, J. A.; Vasquez-Tato, M. P.; Peixoto, F.; Abreu, C. G.; Cidade, H.; Oliveira, A. E.; Pinto, M. *Helv. Chim. Acta* **2008**, *91*, 1336–1345.
- [18] Baker, B. R.; Kozma, J. . *J. Med. Chem.* **1968**, *11*, 656–661.
- [19] Nagahara, K.; Kawano, H.; Sasaoka, S.; Ukawa, C.; Hiramata, T.; Takada, A.; Cottam, H. B.; Robins, R. K. *J. Heterocycl. Chem.* **1994**, *31*, 239–243.
- [20] Miyashita, A.; Iijima, C.; Higashino, T.; Matsuda, H. *Heterocycles* **1990**, *31*, 1309–1314.
- [21] Reddy, K. H.; Reddy, A. P.; Veeranagaiah, V. *Ind. J. Chem. Sec. B* **1992**, *31B*, 163.
- [22] Cheng, C. C.; Robins, R. K. *J. Org. Chem.* **1956**, *21*, 1240–1256.
- [23] Schmidt, P.; Druery, J. *Helv. Chim. Acta* **1956**, *39*, 986–991.
- [24] Tominaga, Y.; Matsuoka, Y.; Oniyama, Y.; Uchimura, Y.; Komiya, H.; Hirayama, M.; Kohra, S.; Hosomi, A. *J. Heterocycl. Chem.* **1990**, *27*, 647–660.
- [25] Davoll, J.; Kerridge, K. A. *J. Chem. Soc.* **1961**, 2589–2591.
- [26] Tominaga, Y.; Hara, M.; Honkawa, Y.; Hosomi, A. *J. Heterocycl. Chem.* **1990**, *27*, 1245–1248.
- [27] Ghozlan, S. A. S.; Abdelrazek, F. M.; Mohamed, M. H.; Azmy, K. E. *J. Heterocycl. Chem.* **2010**, *47*, 1379–1385.
- [28] Neidlein, R.; Wang, Z. *Heterocycles* **1997**, *45*, 1509–1518.
- [29] Seela, F.; Steker, H. *Helv. Chim. Acta* **1986**, *69*, 1602–1613.
- [30] Quiroga, J.; Trilleras, J.; Insuasty, B.; Abonía, R.; Nogueras, M.; Marchal, A.; Cobo,

- J. Tetrahedron Lett.* **2008**, *49*, 3257–3259.
- [31] Slavish, P. J.; Price, J. E.; Hanumesh, P.; Webb, T. R. *J. Comb. Chem.* **2010**, *12*, 807–809.
- [32] Babu, S.; Morrill, C.; Almstead, N. G.; Moon, Y. C. *Org. Lett.* **2013**, *15*, 1882–1885.
- [33] Elion, G. B. *Biosci. Rep.* **1989**, *9*, 509–529.
- [34] Gupta, S.; Rodrigues, L. M.; Esteves, A. P.; Oliveira-Campos, A. M. F.; Nascimento, M. S. J.; Nazareth, N.; Cidade, H.; Neves, M. P.; Fernandes, E.; Pinto, M.; Cerqueira, N. M. F. S. A.; Brás, N. *Eur. J. Med. Chem.* **2008**, *43*, 771–780.
- [35] Honigberg, L. a; Smith, A. M.; Sirisawad, M.; Verner, E.; Loury, D.; Chang, B.; Li, S.; Pan, Z.; Thamm, D. H.; Miller, R. a; Buggy, J. J. *Proc. Natl. Acad. Sci. U. S. A.* **2010**, *107*, 13075–13080.
- [36] Bishop, A. C.; Ubersax, J. a; Petsch, D. T.; Matheos, D. P.; Gray, N. S.; Blethrow, J.; Shimizu, E.; Tsien, J. Z.; Schultz, P. G.; Rose, M. D.; Wood, J. L.; Morgan, D. O.; Shokat, K. M. *Nature* **2000**, *407*, 395–401.
- [37] Mathieu, S.; Gradl, S. N.; Ren, L.; Wen, Z.; Aliagas, I.; Gunzner-Toste, J.; Lee, W.; Pulk, R.; Zhao, G.; Alicke, B.; Boggs, J. W.; Buckmelter, A. J.; Choo, E. F.; Dinkel, V.; Gloor, S. L.; Gould, S. E.; Hansen, J. D.; Hastings, G.; Hatzivassiliou, G.; Laird, E. R.; Moreno, D.; Ran, Y.; Voegtli, W. C.; Wenglowky, S.; Grina, J.; Rudolph, J. J. *Med. Chem.* **2012**, *55*, 2869–2881.
- [38] Curran, K. J.; Verheijen, J. C.; Kaplan, J.; Richard, D. J.; Toral-Barza, L.; Hollander, I.; Lucas, J.; Ayral-Kaloustian, S.; Yu, K.; Zask, A. *Bioorganic Med. Chem. Lett.* **2010**, *20*, 1440–1444.
- [39] Rice, K. D.; Kim, M. H.; Bussenius, J.; Anand, N. K.; Blazey, C. M.; Bowles, O. J.; Canne-Bannen, L.; Chan, D. S. M.; Chen, B.; Co, E. W.; Costanzo, S.; Defina, S. C.; Dubenko, L.; Engst, S.; Franzini, M.; Huang, P.; Jammalamadaka, V.; Khoury, R. G.; Klein, R. R.; Laird, A. D.; Le, D. T.; Mac, M. B.; Matthews, D. J.; Markby, D.; Miller, N.; Nuss, J. M.; Parks, J. J.; Tsang, T. H.; Tshako, A. L.; Wang, Y.; Xu, W. *Bioorganic Med. Chem. Lett.* **2012**, *22*, 2693–2697.
- [40] Díaz, J. L.; Corbera, J.; Cuberes, R.; Contijoch, M.; Enrech, R.; Yeste, S.; Montero, A.; Dordal, A.; Monroy, X.; Almansa, C. *Med. Chem. Commun.* **2017**, *8*, 1235–1245.
- [41] Díaz, J. L.; Corbera, J.; Martínez, D.; Bordas, M.; Sicre, C.; Pascual, R.; Pretel, M. J.; Marín, A. P.; Montero, A.; Dordal, A.; Alvarez, I.; Almansa, C. *Med. Chem. Commun.* **2017**, *8*, 1246–1254.
- [42] Beyzaei, H.; Aryan, R.; Moghaddam-Manesh, M.; Ghasemi, B.; Karimi, P.; Samareh Delarami, H.; Sanchooli, M. *J. Mol. Struct.* **2017**, *1144*, 273–279.
- [43] Ibrahim, S. M.; Abou-Kul, M.; Soltan, M. K.; El-Sayed, A. M. *Int. J. Pharm. Sci. Res.* **2015**, *6*, 3236–3244.
- [44] Massey, V.; Harris, C. M. *Biochem. Soc. Trans.* **1997**, *25*, 750–755.
- [45] Beedham, C. *Prog. Med. Chem.* **1987**, *24*, 85–121.
- [46] Nishino, T.; Okamoto, K.; Eger, B. T.; Pai, E. F.; Nishino, T. *FEBS J.* **2008**, *275*, 3278–3289.
- [47] Cao, H.; Pauff, J. M.; Hille, R. *J. Biol. Chem.* **2010**, *285*, 28044–28053.
- [48] Dobbek, H. *Coord. Chem. Rev.* **2011**, *255*, 1104–1116.
- [49] Pearson, A. R.; Godber, B. L. J.; Eienthal, R.; Taylor, G.; Harrison, R. Image from the RCSB PDB ([www.rcsb.org](http://www.rcsb.org)) of PDB ID 2CKJ <http://www.rcsb.org/pdb/explore/explore.do?structureId=2CKJ> (accessed Aug 29, 2017).
- [50] Enroth, C.; Eger, B. T.; Okamoto, K.; Nishino, T.; Nishino, T.; Pai, E. F. *PNAS* **2000**,

- 97, 10723–10728.
- [51] Hille, R. *Chem. Rev.* **1996**, *96*, 2757–2816.
- [52] Krenitsky, T. A.; Neil, S. M.; Elion, G. B.; Hitchings, G. H. *Arch. Biochem. Biophys.* **1972**, *150*, 585–599.
- [53] Rosemeyer, H.; Seela, F. *Eur. J. Biochem.* **1983**, *134*, 513–515.
- [54] Krenitsky, T. A.; Hall, W. W.; Miranda, P. D. E.; Beauchamp, L. M.; Schaeffer, H. J.; Whitemant, P. D. *Proc. Natl. Acad. Sci. U. S. A.* **1984**, *81*, 3209–3213.
- [55] Shanmuganathan, K.; Koudriakova, T.; Nampalli, S.; Du, J.; Gallo, J. M.; Schinazi, R. F.; Chu, C. K. *J. Med. Chem.* **1994**, *37*, 821–827.
- [56] Reigan, P.; Gbaj, A.; Stratford, I. J.; Bryce, R. A.; Freeman, S. *Eur. J. Med. Chem.* **2008**, *43*, 1248–1260.
- [57] Lee, C.-H.; Han, I.-S. *J. Korean Chem. Soc.* **1992**, *36*, 335–337.
- [58] Pacher, P.; Nivorozhkin, A.; Szabo, C. *Pharmacol. Rev.* **2006**, *58*, 87–114.
- [59] Wang, S. Y.; Yang, C. W.; Liao, J. W.; Zhen, W. W.; Chu, F. H.; Chang, S. T. *Phytomedicine* **2008**, *15*, 940–945.
- [60] Noro, T.; Ueno, A.; Mizutani, M.; Hashimoto, T.; Miyase, T.; Kuroyanagi, M.; Fukushima, S. *Chem. Pharm. Bull.* **1984**, *32*, 4455–4459.
- [61] Van Hoorn, D. E. C.; Nijveldt, R. J.; Van Leeuwen, P. A. M.; Hofman, Z.; M'Rabet, L.; De Bont, D. B. A.; Van Norren, K. *Eur. J. Pharmacol.* **2002**, *451*, 111–118.
- [62] Kumar, R.; Darpan, S. S.; Singh, R. *Expert Opin. Ther. Patents* **2011**, *21*, 1071–1108.
- [63] Schumacher, R. J. *Expert Opin. Investig. Drugs* **2005**, *14*, 893–903.
- [64] Beck, J. R.; Gajewski, R. P.; Hackler, R. E. Xanthine oxidase inhibiting 3(5)-phenyl-substituted-5(3)-pyrazole-carboxylic acid derivatives, compositions, and methods of use. US4495195, 1985.
- [65] Dickinson, C. L.; Williams, J. K.; McKusick, B. C. *J. Org. Chem.* **1964**, *29*, 1915–1919.
- [66] Tolman, R. L.; Robins, R. K.; Townsend, L. B. *J. Am. Chem. Soc.* **1969**, *91*, 2102–2108.
- [67] Cataldo, F.; Lilla, E.; Ursini, O.; Angelini, G. *J. Anal. Appl. Pyrolysis* **2010**, *87*, 34–44.
- [68] Martinez, A. G.; Fernandez, A. H.; Jimenez, F. M.; Martinez, P. J. M.; Martin, C. A.; Subramanian, L. R. *Tetrahedron* **1996**, *52*, 7973–7982.
- [69] Rankovic, Z.; Cai, J.; Kerr, J.; Fradera, X.; Robinson, J.; Mistry, A.; Hamilton, E.; McGarry, G.; Andrews, F.; Caulfield, W.; Cumming, I.; Dempster, M.; Waller, J.; Scullion, P.; Martin, I.; Mitchell, A.; Long, C.; Baugh, M.; Westwood, P.; Kinghorn, E.; Bruin, J.; Hamilton, W.; Uitdehaag, J.; Zeeland, M. van; Potin, D.; Saniere, L.; Fouquet, A.; Chevallier, F.; Deronzier, H.; Dorleans, C.; Nicolai, E. *Bioorg. Med. Chem. Lett.* **2010**, *20*, 1524–1527.
- [70] Takahashi, Y.; Hibi, S.; Hoshino, Y.; Kikuchi, K.; Shin, K.; Murata-Tai, K.; Fujisawa, M.; Ino, M.; Shibata, H.; Yonaga, M. *J. Med. Chem.* **2012**, *55*, 5255–5269.
- [71] Murphy, R. C.; Ojo, K. K.; Larson, E. T.; Castellanos-Gonzalez, A.; Perera, B. G. K.; Keyloun, K. R.; Kim, J. E.; Bhandari, J. G.; Muller, N. R.; Verlinde, C. L. M. J.; White, A. C.; Merritt, E. A.; Van Voorhis, W. C.; Maly, D. J. *ACS Med. Chem. Lett.* **2010**, *1*, 331–335.
- [72] Dally, R. D.; Huang, J.; Joseph, S.; Sheperd, T. A.; Holst, C. L. p70 S6 Kinase Inhibitors. WO 2008/140947 A1, 2008.
- [73] Maxwell, B. D.; Boyé, O. G.; Ohta, K. *J. Label. Compd. Radiopharm.* **2005**, *48*, 397–406.



- [74] Arsianti, A.; Hanafi, M.; Saepudin, E.; Morimoto, T.; Kakiuchi, K. *Bioorg. Med. Chem. Lett.* **2010**, *20*, 4018–4020.
- [75] Pace, P.; Di Francesco, M. E.; Gardelli, C.; Harper, S.; Muraglia, E.; Nizi, E.; Orvieto, F.; Petrocchi, A.; Poma, M.; Rowley, M.; Scarpelli, R.; Laufer, R.; Paz, O. G.; Monteagudo, E.; Bonelli, F.; Hazuda, D.; Stillmock, K. A.; Summa, V. *J. Med. Chem.* **2007**, *50*, 2225–2239.
- [76] Bunting, J. W.; Luscher, M. A.; Redman, J. *Bioorg. Chem.* **1987**, *15*, 125–140.
- [77] Kažoka, H.; Madre, M. *Talanta* **2005**, *67*, 98–102.
- [78] Kažoka, H. *J. Chromatogr. A* **2008**, *1189*, 52–58.
- [79] Earl, R. A.; Pugmire, R. J.; Revankar, G. R.; Townsend, L. B. *J. Org. Chem.* **1975**, *40*, 1822–1828.
- [80] Hecht, S. M.; Werner, D.; Traficante, D. D.; Sundaralingam, M.; Prusiner, P.; Ito, T.; Sakurai, T. *J. Org. Chem.* **1975**, *40*, 1815–1822.

## 7 Appendix

### List of Abbreviations

ACIB	Austrian Center for Industrial Biotechnology
ACN	Acetonitrile
B-Raf	B-rapidly accelerated fibrosarcoma
Btk	Bruton tyrosine kinase
DCM	Dichloromethane
DMF	Dimethylformamide
DMSO- <i>d</i> 6	Deuterated dimethyl sulfoxide
FAD	Flavin adenine dinucleotide
HPLC	High performance liquid chromatography
IC50	Half maximal inhibitory concentration
MAOS	Microwave assisted organic synthesis
mTOR	Mammalian target of rapamycin
NAD	Nicotinamide adenine dinucleotide
NMR	Nuclear magnetic resonance
p-TSA	<i>p</i> -Toluenesulfonic acid
p70S6K	Ribosomal protein S6 kinase beta-1
RP	Reversed phase
SFKs	Src family kinases
TBAI	Tetrabutylammonium iodide
TEA	Triethylamine
TFAA	Trifluoroacetic anhydride
THF	Tetrahydrofuran
TLC	Thin layer chromatography
TP	Thymidine phosphorylase
XDH	Xanthine dehydrogenase
XO	Xanthine oxidase

### List of Schemes

Scheme 1. Example of a synthesis scheme used in the preparation of the targeted compounds.....	3
Scheme 2. Robins path to 1,2-unsubstituted pyrazolo[3,4- <i>d</i> ]pyrimidines; (i) NH <sub>2</sub> NH <sub>2</sub> , EtOH, reflux; (ii) HCONH <sub>2</sub> , reflux; (iii) NH <sub>2</sub> CONH <sub>2</sub> , 180-200°C; (iv)NH <sub>2</sub> CSNH <sub>2</sub> , 180°C .....	6
Scheme 3. Synthesis of 6-phenylamino-substituted pyrazolo[3,4- <i>d</i> ]pyrimidines; (i) PPh <sub>3</sub> , Br <sub>2</sub> , TEA, 0-25°C; (ii) phenyl isocyanate, THF, 25°C; (iii) NH <sub>3</sub> , THF, rT; (iv) MeOH, reflux.....	7

Scheme 4. Synthesis of 4-amino-3-cyanomethylpyrazolo[3,4- <i>d</i> ]pyrimidines; (i) $(\text{EtO})_3\text{CH}$ , $\text{Ac}_2\text{O}$ , $140^\circ\text{C}$ ; (ii) $\text{NH}_3/\text{EtOH}$ , rT	8
Scheme 5. Bulychevs approach to 3-cyano-4-amio-pyrazolo[3,4- <i>d</i> ]pyrimidines; (i) dimethylformamide diethylacetal, MeOH abs., reflux temperature; (ii) $\text{NH}_4\text{OH}$ 20%, reflux....	8
Scheme 6. Syntheses starting from pyrazole variant A; (i) reflux; (ii) $\text{H}_2\text{O}_2$ , KOH, $75^\circ\text{C}$ ; (iii) $\text{NH}_3/\text{MeOH}$ , $200^\circ\text{C}$ ; (iv) $\text{CH}_3\text{COONa}$ , $200^\circ\text{C}$ .....	9
Scheme 7. Syntheses starting from pyrazole variant B; (i) AcOH, rT ; (ii) HCl or p-TSA, MeOH, reflux; (iii) DMF, reflux; (iv) $\text{C}_2\text{H}_5\text{ONa}$ , EtOH, reflux .....	10
Scheme 8. Slavishs approach using a pyrimidine precursor; (i) $\text{RNH}_2$ , $\text{KHCO}_3$ , TBAI, DCM or THF/ $\text{H}_2\text{O}$ , rT; (ii) $\text{R}_1\text{NH}_2$ , $\text{KHCO}_3$ , TBAI, DCM/ $\text{H}_2\text{O}$ , rT; (iii) $\text{R}_2\text{NHNH}_2$ , THF, reflux.....	12
Scheme 9. The last two steps of the purine catabolism; Oxidation of Hypoxanthine to uric acid .....	17
Scheme 10. General reaction scheme of molybdenum hydroxylases .....	20
Scheme 11. Reaction mechanism of Xanthine oxidase <sup>[47]</sup> .....	20
Scheme 12. Proposed synthesis route to pyrazolo[3,4- <i>d</i> ]pyrimidines (1) and (2).....	26
Scheme 13. Synthesis of pyrazole precursor (7); (i) semicarbazide hydrochloride, EtOH, triethylamine, $0^\circ\text{C}$ ; (ii) boiling $\text{H}_2\text{O}$ dest.....	27
Scheme 14. Synthesis approach to (1) published by Taylor and Abul-Husn; (i) triethyl orthoformate, reflux, inert atmosphere ( $\text{N}_2$ ), 7 h; (ii) EtOH, ethanolic ammonia (saturated at $0^\circ\text{C}$ ), r.t., 24 h.....	27
Scheme 15. Pyrrolopyrimidine synthesis by Tolman et al.; (i) ethoxy ethanol, reflux, 36 h....	28
Scheme 16. Proposed synthesis route to pyrazolopyrimidine (1) starting from 2-[Bis(methylthio)methylene]malononitrile .....	31
Scheme 17. Synthesis of 4-amino-3-methylthiopyrazolo[3,4- <i>d</i> ]pyrimidine; (i) MeOH, reflux temperature, 2 h; (ii) reflux temperature, 12 h.....	32
Scheme 18. Bulychevs approach to pyrazolopyrimidine (1); (i) MeOH abs., reflux temperature; (ii) $\text{NH}_4\text{OH}$ 20 %, reflux.....	35
Scheme 19. Synthesis route to targeted pyrazolopyrimidines (3), (4), and (5) .....	38

Scheme 20. Synthesis of 4-aminopyrazolo[3,4- <i>d</i> ]pyrimidine (3); (i) reflux temperature, 45 min; (ii) 180 °C, 8 h, inert atmosphere .....	38
Scheme 21. Conversion of 4-pyrimidinone by XO .....	48

## List of Figures

Figure 1. (i) purine scaffold; (ii) pyrazolo[3,4- <i>d</i> ]pyrimidine scaffold.....	3
Figure 2. 1 <i>H</i> -pyrazolo[3,4- <i>d</i> ]pyrimidine .....	5
Figure 3. Numbering of the pyrazolopyrimidine system and its main compounds .....	5
Figure 4. Different substituents used to build up the pyrimidine moiety.....	7
Figure 5. (i) Allopurinol; (ii) Oxypurinol.....	13
Figure 6. Structure of XO-inhibitors synthesized by Gupta et al.....	14
Figure 7. Pyrazolo[3,4- <i>d</i> ]pyrimidines inhibiting various types of enzymes; (i) Ibrutinib; Btk <sup>[35]</sup> (ii) 1NM-PP1; SFKs <sup>[36]</sup> (iii) -; B-Raf <sup>[37]</sup> (iv) WYE-132; mTOR <sup>[38]</sup> (v) XL418; p70S6K <sup>[39]</sup> 15	
Figure 8. 3D image of human milk Xanthine oxidase <sup>[49]</sup> .....	18
Figure 9. Structures of the molybdenum cluster in the XO active site (i) and the pyranopterin cofactor (ii) .....	19
Figure 10. Stereoview on the active site of Xanthine oxidoreductase with bound Hypoxanthine <sup>[48]</sup> .....	19
Figure 11. Condensed heterocyclic substrates of XO with their corresponding reaction rates; (i) 4-oxopyrido[3,2- <i>d</i> ]pyrimidine; (ii) Xanthine; (iii) Hypoxanthine; (iv) purine; (v) 4-oxopteridine (vi) Allopurinol; (vii) 4-oxopyrido[2,3- <i>d</i> ]pyrimidine; (viii) Pteridine; (ix) 7-oxotriazolo[4,5- <i>d</i> ]pyrimidine; (x) pyrazolo[3,4- <i>d</i> ]pyrimidine; (xi) Quinazoline; (xii) triazolo[4,5- <i>d</i> ]pyrimidine.....	22
Figure 12. Examples of prodrug activation using XO .....	23
Figure 13. (i) Allopurinol; (ii) Cinnamaldehyde; (iii) norathyriol; (iv) Apigenin; (v) Febuxostat; (vi) 4-hydroxy-3-(4-(trifluoromethyl)phenyl)-1 <i>H</i> -pyrazole-5-carboxylic acid .....	25

Figure 14. Targeted pyrazolo[3,4- <i>d</i> ]pyrimidines.....	26
Figure 15. HPLC chromatograms of the treatment of the condensation reaction using formamide with NH <sub>3</sub> aq., HPLC method 2.....	30
Figure 16. HPLC chromatogram after the oxidation screening, variants (A) and (C); UV signals at 275.8nm; HPLC method 2 .....	33
Figure 17. <sup>13</sup> C-NMR spectrum of 4-amino-3-methylsulfonylpyrazolo[3,4- <i>d</i> ]pyrimidine.....	33
Figure 18. HPLC chromatogram of the sulfone-cyano exchange; (A) scan mode; (B) reactant (sulfone) sim; (C) product sim; HPLC method 2.....	34
Figure 19. HPLC chromatogram of compound (14); (A) scan mode; (B) sim mode; (C) UV signal at 275.8nm; HPLC method 3.....	36
Figure 20. <sup>13</sup> C-NMR spectrum of 4-amino-3-cyano-1 <i>H</i> -pyrazolo[3,4- <i>d</i> ]pyrimidine (1) .....	36
Figure 21. <sup>13</sup> C-NMR spectrum of 3-cyano-4-oxo-1 <i>H</i> -pyrazolo[3,4- <i>d</i> ]pyrimidine (2) .....	37
Figure 22. <sup>13</sup> C-NMR spectrum of 4-aminopyrazolo[3,4- <i>d</i> ]pyrimidine (3).....	39
Figure 23. <sup>1</sup> H-NMR spectrum of Allopurinol (4).....	39
Figure 24. HPLC chromatogram of Allopurinol; (A) sim mode; (B) UV signal at 250.8nm; HPLC method 4.....	40
Figure 25. HPLC chromatogram of the first chlorination attempt; (A) sim mode m/z ratio compound (5); (B) UV signal 265.8nm; HPLC method 4.....	41
Figure 26. TLC chromatogram of the first enzymatic conversion; (R1) c Xanthine 0.72 mM, c enzyme 1.96 g/10 ml; (R2) c Xanthine 0.72 mM, c enzyme 1 g/10 ml; (R3) c Xanthine 0.72 mM, c enzyme 0.5 g/10 ml; (SB) substrate blank; (EB) enzyme blank.....	43
Figure 27. possible small molecule targets for XO; (i) 2-cyanopyridine; (ii) 3-cyanopyridine; (iii) 2-cyanopyrazine; (iv) 2-cyanopyrimidine; (v) 2-cyanopyrrole; (vi) Xanthine.....	44
Figure 28. HPLC chromatogram of the XO conversion of 2-cyanopyridine; (A) reaction with c enzyme 1.96 g/ 10 ml; (B) reaction with c enzyme 0.5 g/ 10 ml; (C) substrate blank; (D) enzyme blank c enzyme 1.96 g/ 10 ml; HPLC method 5.....	45
Figure 29. HPLC chromatogram of Xanthine and uric acid; UV signal at 262.8 nm; HPLC method 8.....	46

Figure 30. HPLC chromatogram of Xanthine and uric acid in the buffer system; UV signal at 270.8 nm; HPLC method 9 .....	46
Figure 31. HPLC chromatogram of XO conversion reaction during the development of a positive control for the activity test; (A) substrate blank; (B) enzyme blank; (C) conversion; UV signals at 270.8 nm; HPLC method 9 .....	47
Figure 32. HPLC chromatogram of 4-pyrimidinone on the LiChrospher® 100 DIOL column; HPLC-method 10.....	48
Figure 33. HPLC chromatogram of uracil and 4-pyrimidinone; HPLC method 11.....	49
Figure 34 Synthesized targeted pyrazolo[3,4- <i>d</i> ]pyrimidines.....	50
Figure 35 Pyrazolo[3,4- <i>d</i> ]pyrimidines synthesized additionally to the targeted compounds ..	50

## List of Tables

Table 1. Overview of reactants and corresponding pyrazole precursors .....	11
Table 2. overview oxidation screening.....	32